Ontario

We are committed to providing accessible customer service.
If you need accessible formats or communications supports, please contact us.

Nous tenons à améliorer l'accessibilité des services à la clientèle.
Si vous avez besoin de formats accessibles ou d'aide à la communication, veuillez nous contacter.

Technical Report: 2020 Airborne Geophysical Program

On the KWAI Property
UTM ZONE 15, GCS: NAD 1983
454500, 5622000
NTS 52K/12-13

PREPARED BY: GORDEY, E., MACKAY, G.
REPORT COMPLETED DATE, 2022-03-10

Table of Contents

Figures

Tables

SUMMARY

This report presents and summarizes the results of the ***2020 Airborne Geophysical work program*** on the Kwai property, as per the requirements of ENDM's 2018 Technical standard on Assessment work Reporting. The report is organized with property introduction including location and access, previous exploration work, regional geology, and, property geology. All work was conducted on the Kwai property, in the Cabin Bay and Dixie Lake areas of the Red Lake Mining District. The 2020 airborne geophysics program was conducted on behalf of Golden Goliath Resources Ltd. by Terraquest Ltd. based in Ontario. Claim locations and coordinates were provided to Terraquest from the MLAS operational tenure data supported by Lands Information System Ontario (LIO). All tie points, corners points and flight lines were prepared using NAD 1983 UTM Zone 15N (refer to Appendix B, section 2.3-Navigation Specifications, Pg 6-7.)

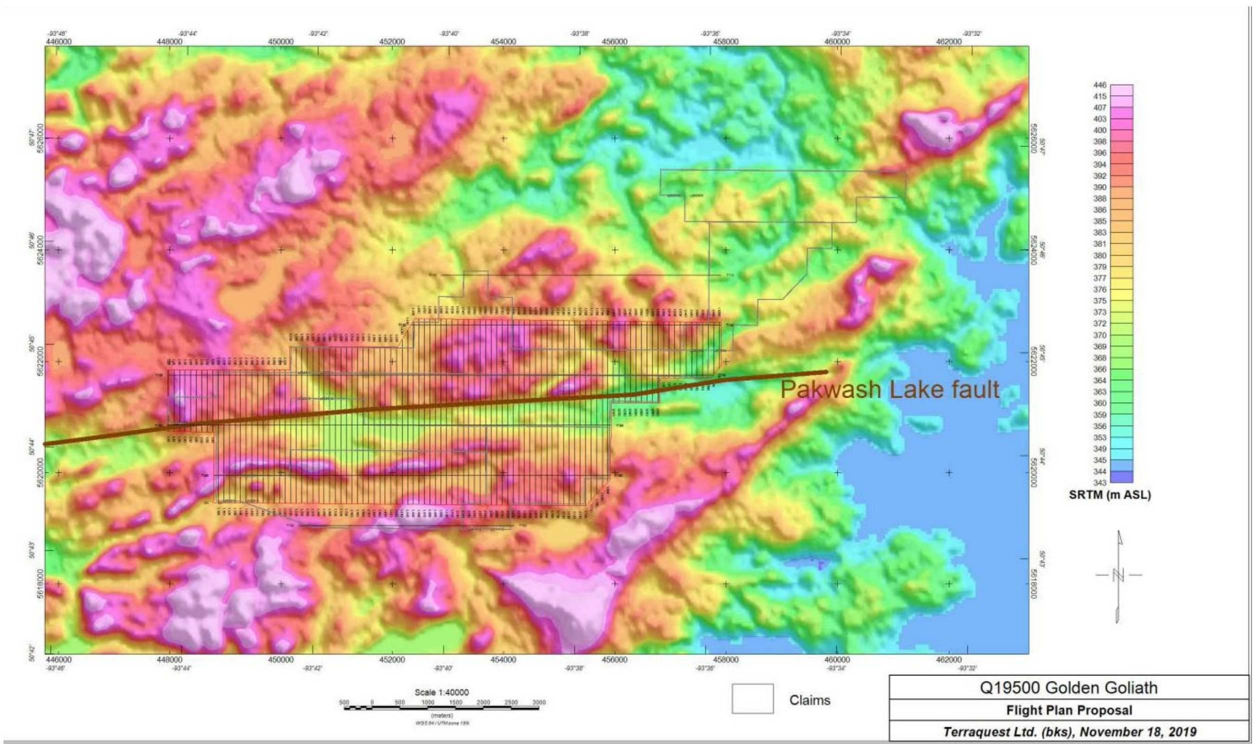

CONCLUSIONS OF SURVEY

High resolution horizontal gradient magnetic data have provided a detailed data set which can be used to improve the magnetic mapping. The Matrix VLF-EM total field products show good correlation with both magnetic and geologic trends and have been successful in identifying and mapping the structural fabric across the survey area. The Matrix VLF-EM data have been inverted to obtain resistivity data channels, grids and map images of depth slices of the inverted VLF-EM, plus voxels to enable 3D viewing of the VLF-EM Resistivity interpretation.

RECOMMENDATIONS

1. A program of geological mapping at 1:10000 scale to better tie the geophysics into the property geology.
2. Ground geophysics using induced polarization to identify areas of chargeability associated with the structures shown on the VLF.
3. Diamond drilling program to test priority targets.

PROPERTY IDENTIFICATION

LOCATION AND ACCESS

The Kwai property is in the Red Lake area, approximately 38 kilometres south of Red Lake and 30 kilometers west of Ear Falls, in the Red Lake Mining Division, NTS sheet 52K/12 and 52K/13. Access on to the property was by truck on the Dixie Lake Forest Road which crosses the northern portion of the property (see figure 4: Kwai Property Scale Map). Within the property, access is by truck and ATV on secondary and tertiary forest roads maintained by the Red Lake Forest Company working under the Algoma Forest Management Unit. The Dixie Lake Forest road crosses onto the Kwai property ~13km south of junction with Highway 105. The junction at highway 105 is ~35 kilometers northwest of Ear Falls.

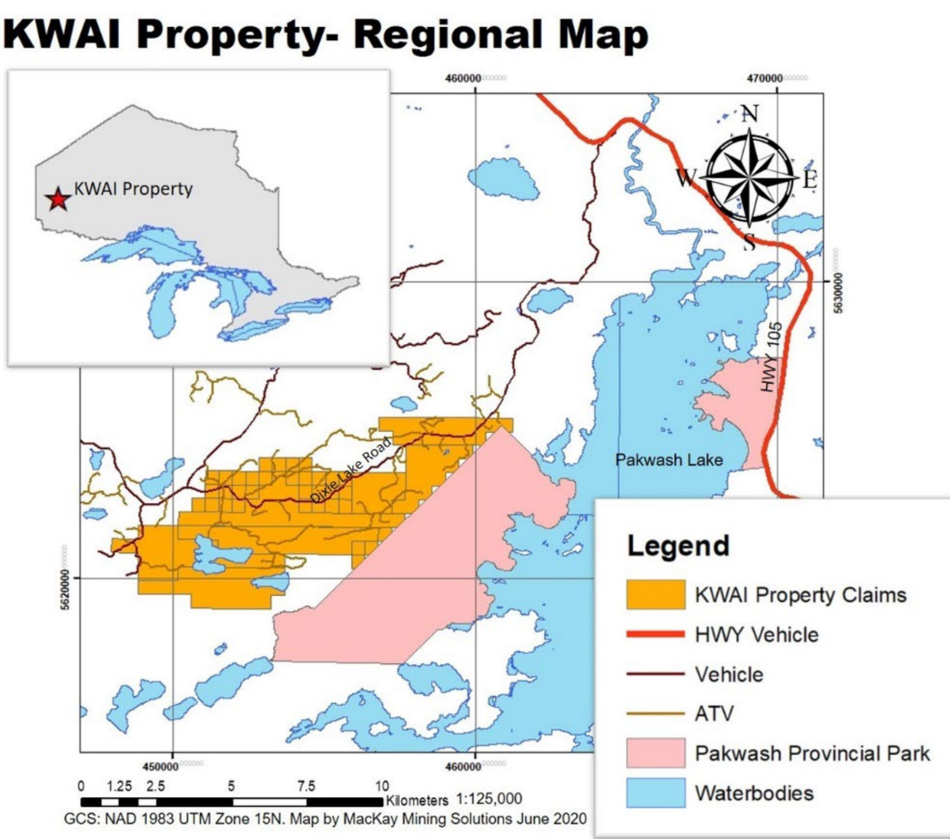

CLAIMS AND CURRENT OWNERSHIP

In 2020 the Kwai property consists of 41 contiguous staked single and multi-cell claims (164 cells), comprising approximately 3,800 hectares (Figure 3). Table 1 below contains claim and cell tenure status for the claims included in the airborne geophysics survey program. The program included 20 single and multicell claims or 116 cells.

Property	Township/Area	Tenure ID	Cell Unit Key	Anniversary	Annual Work Required	Total Reserve
KWAI	Cabin Bay Area	530311	52K13B355	2022-08-28	$400.00	
			52K13B374		$400.00	
			52K13B375		$400.00	
			52K13B376		$400.00	
			52K13B393		$400.00	
			52K13B394		$400.00	
			52K13B395		$400.00	
			52K13B396		$400.00	
			52K12J008		$400.00	
			52K12J009		$400.00	
			52K12J010		$400.00	
			52K12J011		$400.00	
			52K12J012		$400.00	
			52K12J013		$400.00	
			52K12J014		$400.00	
			52K12J015		$400.00	
			52K12J016		$400.00	
			52K12J017		$400.00	
			52K12J018		$400.00	
			52K12J019		$400.00	
			52K12J020		$400.00	
			52K12L001		$400.00	
			52K12L002		$400.00	
			52K12L003		$400.00	
			52K12L004		$400.00	$779
KWAI	Cabin Bay Area	530312	52K12J028	2020-08-29	$400.00	
			52K12J029		$400.00	
			52K12J030		$400.00	
			52K12J031		$400.00	
			52K12J032		$400.00	
			52K12J033		$400.00	
			52K12J034		$400.00	
			52K12J035		$400.00	

			52K12J036		$400.00	
			52K12J037		$400.00	
			52K12J038		$400.00	
			52K12J039		$400.00	
			52K12J040		$400.00	
			52K12J051		$400.00	
			52K12J052		$400.00	
			52K12J053		$400.00	
			52K12J054		$400.00	
			52K12J055		$400.00	
			52K12J056		$400.00	
			52K12J057		$400.00	
			52K12J058		$400.00	
			52K12J059		$400.00	
			52K12J060		$400.00	
			52K12L021		$400.00	
			52K12L022		$400.00	$1,917
KWAI	Cabin Bay/Dixie Lake Area	**530908**	52K13A305	2022-09-06	$400.00	
			52K13A306		$400.00	
			52K13A307		$400.00	
			52K13A308		$400.00	
			52K13A309		$400.00	
			52K13A325		$400.00	
			52K13A326		$400.00	
			52K13A327		$400.00	
			52K13A328		$400.00	
			52K13A345		$400.00	
			52K13A346		$400.00	
			52K13A347		$400.00	
			52K13A365		$400.00	
			52K13A366		$400.00	
			52K13A384		$400.00	
			52K13A385		$400.00	$0.00
KWAI	Cabin Bay/Dixie Lake Area	**530909**	52K12J025	2022-09-06	$400.00	
			52K12J026		$400.00	
			52K12J027		$400.00	
			52K12J043		$400.00	
			52K12J044		$400.00	
			52K12J045		$400.00	
			52K12J046		$400.00	
			52K12J047		$400.00	
			52K12J048		$400.00	
			52K12J049		$400.00	

			52K12J050		$400.00	
			52K12J065		$400.00	
			52K12J066		$400.00	
			52K12J067		$400.00	
			52K12J068		$400.00	
			52K12J069		$400.00	
			52K12J070		$400.00	
			52K12J071		$400.00	
			52K12J072		$400.00	
			52K12J073		$400.00	
			52K12J074		$400.00	
			52K12J075		$400.00	
			52K12J085		$400.00	
			52K12J086		$400.00	
			52K12J087		$400.00	$5,762
KWAI	Cabin Bay/Dixie Lake Area	**530910**	52K12J088	2022-09-06	$400.00	
			52K12J089		$400.00	
			52K12J090		$400.00	
			52K12J091		$400.00	
			52K12J092		$400.00	
			52K12J093		$400.00	
			52K12J094		$400.00	
			52K12J095		$400.00	
			52K12J105		$400.00	
			52K12J106		$400.00	
			52K12J107		$400.00	
			52K12J108		$400.00	
			52K12J109		$400.00	
			52K12J110		$400.00	
			52K12J111		$400.00	
			52K12J112		$400.00	
			52K12J113		$400.00	
			52K12J114		$400.00	
			52K12J115		$400.00	
			52K12J129		$400.00	
			52K12J130		$400.00	
			52K12J131		$400.00	
			52K12J132		$400.00	
			52K12J133		$400.00	
			52K12J134		$400.00	$0.00
KWAI	Cabin Bay/Dixie Lake	**543033**	52K13B389	2023-02-21	$400.00	$0.00
KWAI	Cabin Bay/Dixie Lake	**543034**	52K13B390	2023-02-21	$400.00	$0.00
KWAI	Cabin Bay/Dixie Lake	**543035**	52K13B391	2023-02-21	$400.00	$0.00

KWAI	Cabin Bay/Dixie Lake	543036	52K13B392	2023-02-21	$400.00	$0.00
KWAI	Cabin Bay/Dixie Lake	543039	52K13B372	2023-02-21	$400.00	$0.00
KWAI	Cabin Bay/Dixie Lake	543040	52K13B373	2023-02-21	$400.00	$0.00
KWAI	Cabin Bay/Dixie Lake	543051	52K13B377	2023-02-21	$400.00	$0.00
KWAI	Cabin Bay/Dixie Lake	543052	52K13B378	2023-02-21	$400.00	$0.00
KWAI	Cabin Bay/Dixie Lake	543053	52K13B379	2023-02-21	$400.00	$0.00
KWAI	Cabin Bay/Dixie Lake	543054	52K13B380	2023-02-21	$400.00	$0.00
KWAI	Cabin Bay/Dixie Lake	543055	52K13B397	2023-02-21	$400.00	$0.00
KWAI	Cabin Bay/Dixie Lake	543056	52K13B398	2023-02-21	$400.00	$0.00
KWAI	Cabin Bay/Dixie Lake	543057	52K13B399	2023-02-21	$400.00	$0.00
KWAI	Cabin Bay/Dixie Lake	543058	52K13B400	2023-02-21	$400.00	$0.00
KWAI	Cabin Bay/Dixie Lake	550975	52K13A341	2022-05-29	$400.00	
			52K13A342		$400.00	
			52K13A343		$400.00	
			52K13A344		$400.00	
			52K13A361		$400.00	
			52K13A362		$400.00	
			52K13A363		$400.00	
			52K13A364		$400.00	
			52K13A381		$400.00	
			52K13A382		$400.00	
			52K13A383		$400.00	$0.00

Table 1: KWAI Property: Claims and cells where work was performed updated 2022-03-01

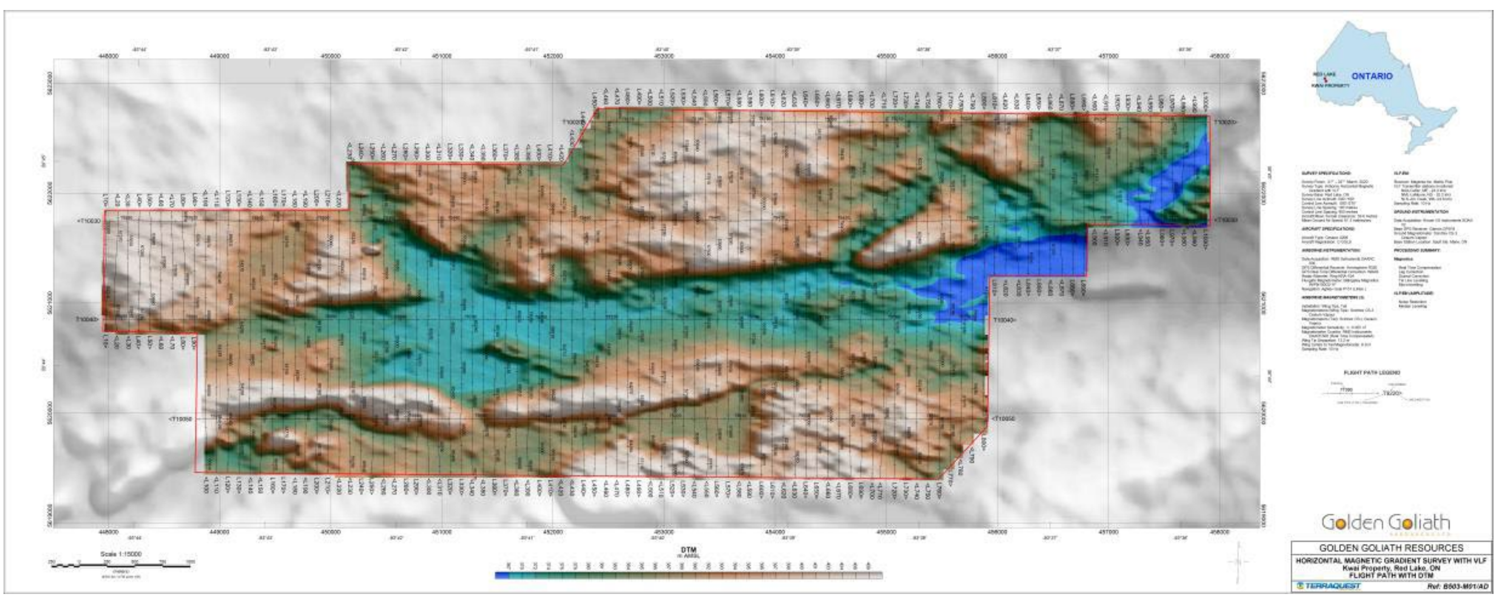

Figure 3: Airborne Survey Flight Path over Digital Elevation Model

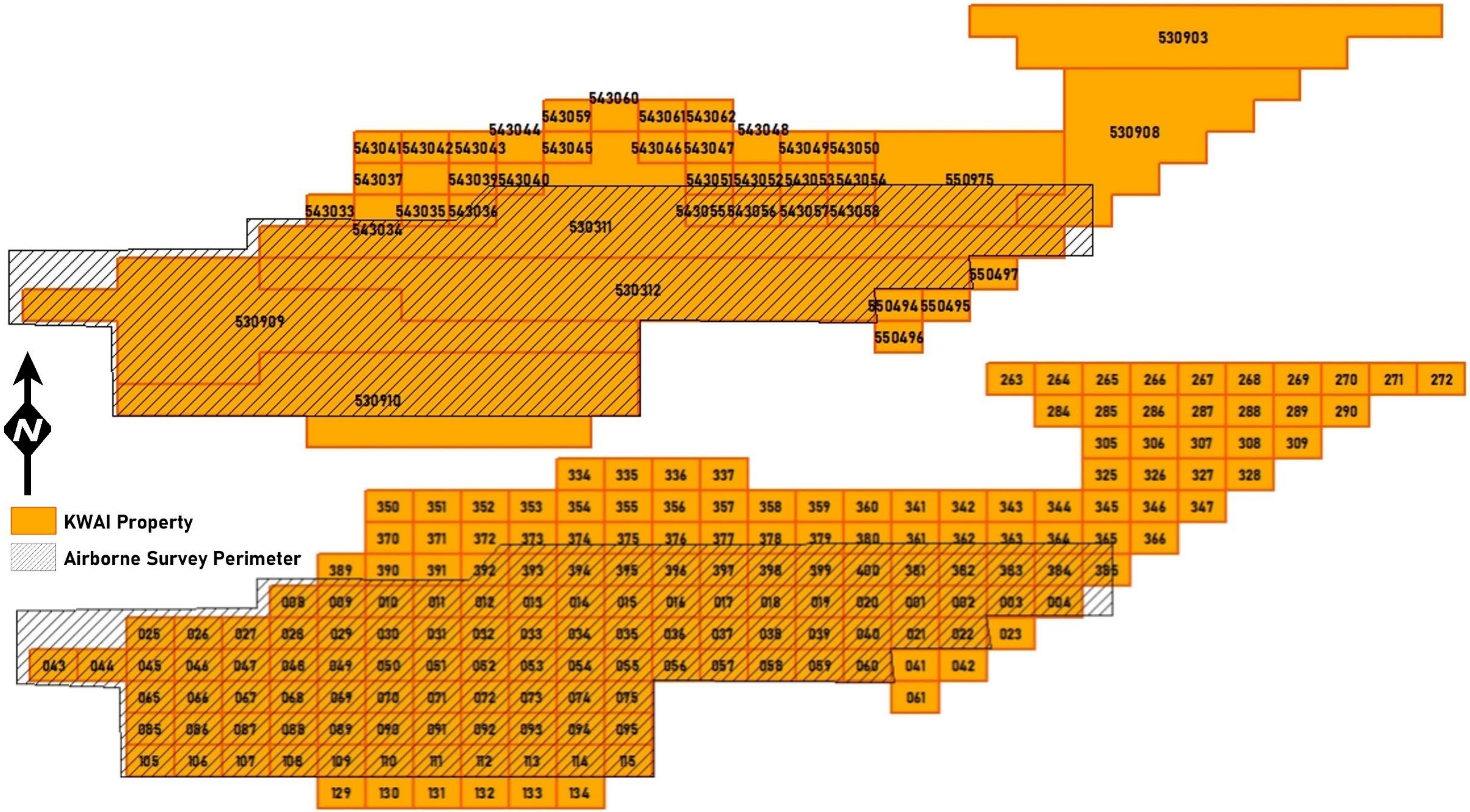

Figure 4: KWAI Work Program- Claim and Cell View NAD 1983 CSRS

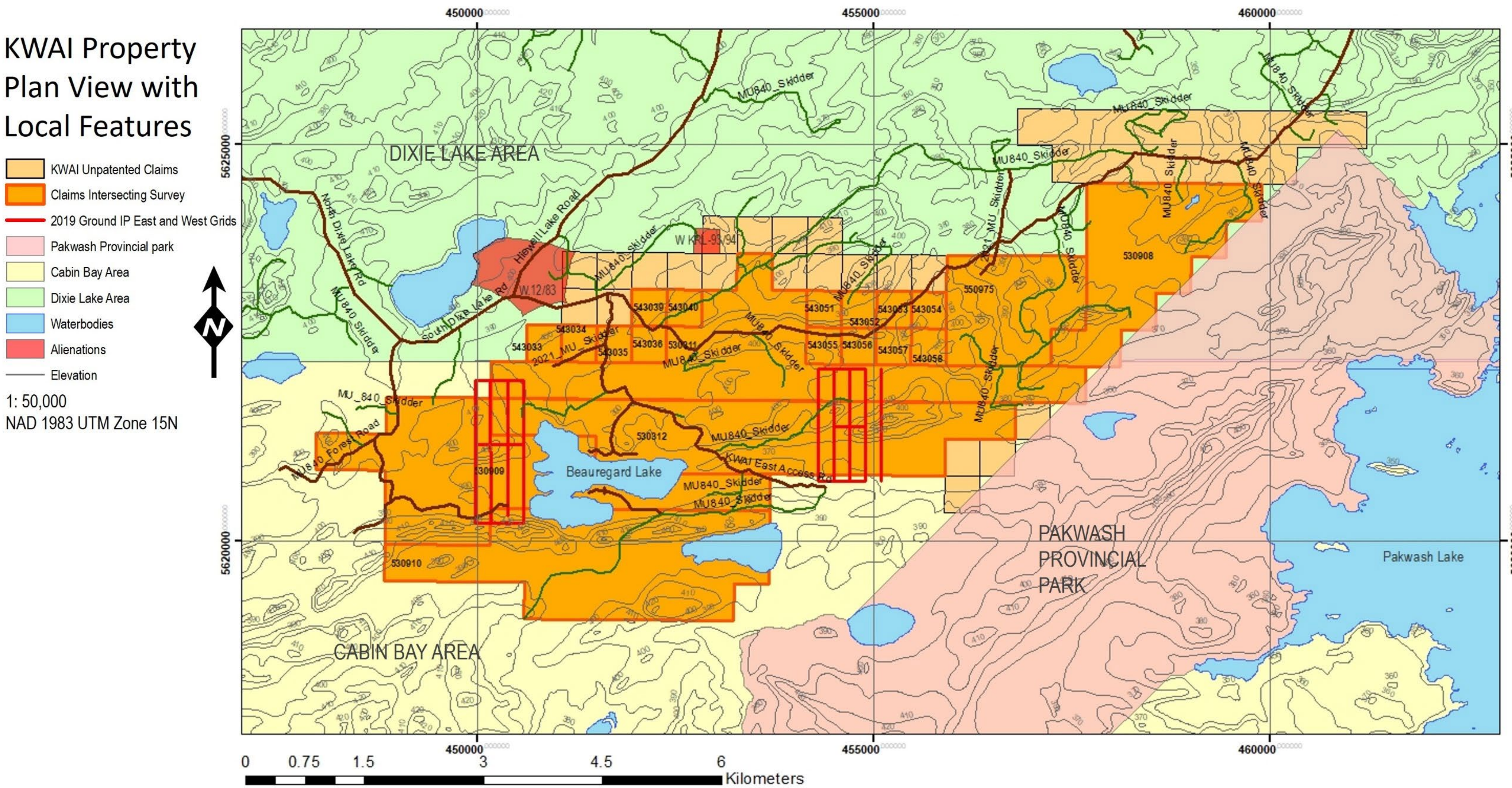

Figure 5: KWAI Property Scale Map with Local Features

PROPERTY HISTORY

PREVIOUS WORK

The Kwai Property has no documented exploration previous to the work by Laurentian Goldfields Ltd. described below, according to the data available in the assessment files archived with the Ontario Ministry of Energy, Northern Development and Mines on the MENDM website: (www.geologyontario.mndm.gov.on.ca/). Most of the previous work in the area has focused on the Dixie Zone area currently being explored by Great Bear Resources and BTU Metals, about 10 km to the north.

2010: Laurentian Goldfields Ltd. staked a large property (approximately 22,940 ha) in the area from December 2009 to January 2010 following the delineation of a large hydrogeochemical anomaly over Pakwash Lake. The property was several times the size of the current Property and most of it was not covered by the current Property.

Initial work on the property consisted of a high resolution, airborne magnetic and VLF- EM survey completed in March 2010. Phase 2 of the project included comprehensive soil and lake sediment sampling as well as a property-wide mapping and prospecting program, which systematically targeted structures and lithological contacts interpreted from magnetic susceptibility mapping.

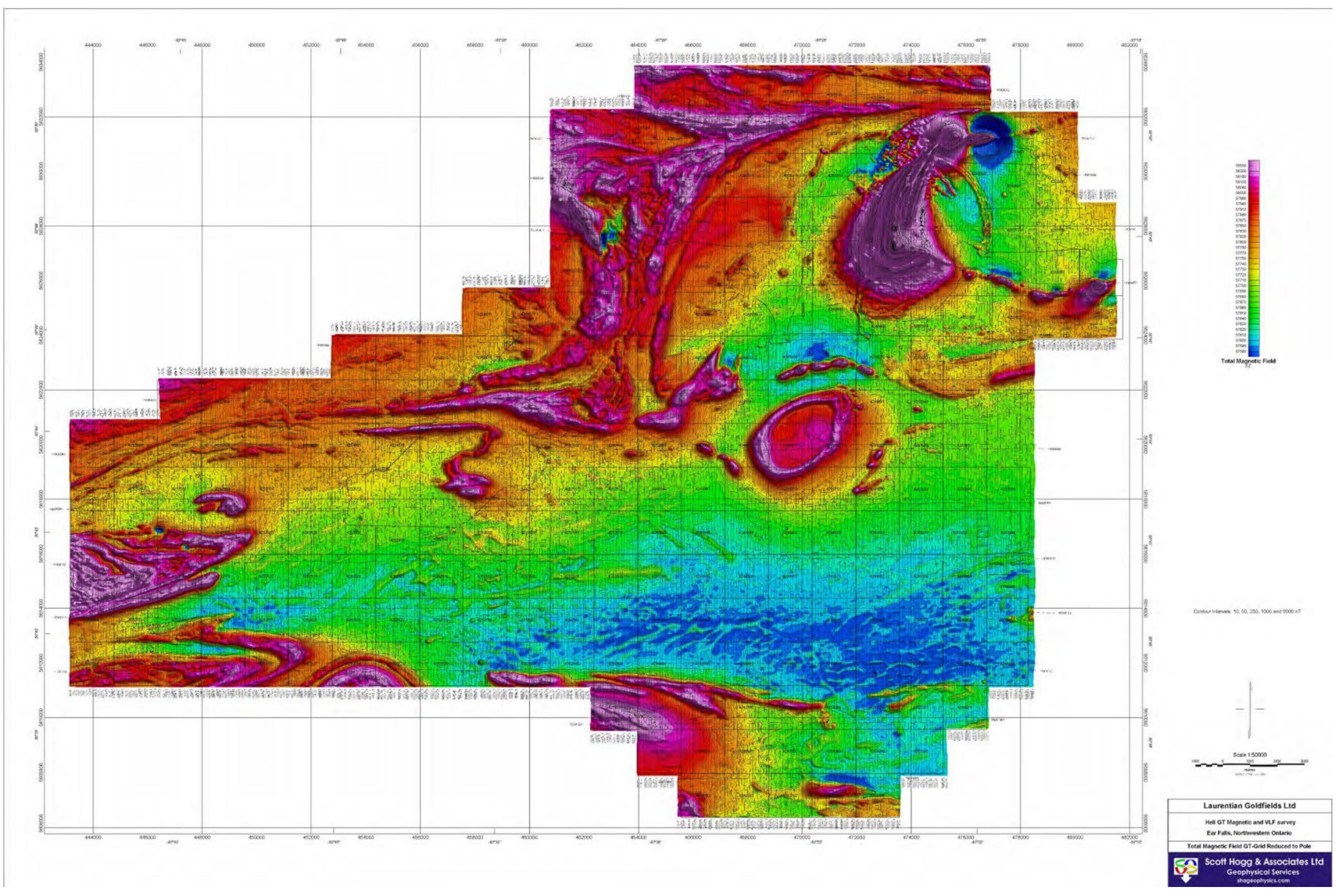

Figure 6: Historical Laurentian Goldfields Airborne Mag and VLF Survey

Prospecting in the western portion of the property recovered slightly anomalous Au samples from within the granodiorite pluton. A grab sample of a pyrite-bearing quartz vein occurring in the granodiorite contained 243ppb Au. Fifty six (56) channel samples were reportedly collected from the nearby Kwai trench on Golden Goliath's Property, (Render et al. 2010), however, the assays and certificates for these samples were not included in Laurentian's 2010 report, and therefore the authors cannot report on any of the results.. This area also reported "some of the most extensive high gold response ratio anomalies defined by the detailed MMI (mobile metal ion) soil sampling survey."[1]

2011: In the winter of 2011, Laurentian drilled 9 holes on the ice on Pakwash Lake to test a large lake sediment gold and pathfinder element anomaly, however this part of their property is not covered by the current Property, and of 836 samples taken for assay, the high value was 40 ppb, with the rest averaging slightly above detection limit.[2]

The drill program was followed up by further MMI soil sampling and rock sampling over nine grids on their property, including over the Kwai area on Golden Goliath's Property. The purpose of this sampling was to better define the anomalies by sampling on tighter spacing in order to infill the wider spaced sampling done in 2010. The work was reported to have helped in further defining the gold mineralization in the Kwai area, although it was stated that further work was required to "validate these targets to drilling status."[3]

2012: In the fall of 2012 Laurentian conducted further soil and rock sampling utilizing three different analytical methods as provided by Acme Analytical Laboratories; an ultratrace method with aqua regia digestion, partial leaching with sodium pyrophosphate and leaching with distilled water. The work was reported to be successful in validating the occurrence of the gold anomaly in the Kwai area, and further mapping and surface sampling of the Kwai area to better define subsurface targets was recommended as well as trenching in areas of limited glacial cover (Chiang and Labrenz, 2013). They also recommended drill testing of selected targets with wide-spaced shallow holes to test for large-scale alteration and/or mineralization.

2019:

Following compilation of previous work on the property an initial property assessment was conducted in June of 2019.

The trace of the Pakwash fault seen in the airborne magnetics from Laurentian Goldfields was confirmed on the ground as a clear break in topography. On the south side of the break there are

[1] Render, M., Meade, S.R., Lengyel, J.W.P., 2011. Goldpines North Property Drilling Report, Ear Falls Area, Ontario, Canada; *prepared for* Laurentian Goldfields Ltd. AFRI 20011328.

[2] Render et al. (2011)

[3] Chiang, M., and Rennie, C., 2013. Goldpines North Property Summer 2011 Exploration Report, Ear Falls Area, Ontario, Canada; *prepared for* Laurentian Goldfields Ltd. AFRI 20011980

no outcrop exposures. However, on the north side Uchi formation mafic volcanics were seen in contact with the granodiorite.

The very weak soil Geochem responses seen in the Laurentian Goldfields work may be explained by a pervasive blanket of silt from glacial lake Agassiz which appears to cover much of the property.

Two breaks identified along the magnetic trend of the Pakwash fault were selected for a program of ground geophysics. 9 lines of IP were done north south across the structure on two grids ~4 kilometers apart.

Ground Geophysics:

The IP survey was successful in outlining several areas of interest across the survey portion of the two grids. The main IP target areas on both grids appear to correlate to the suspected main fault zone, The Pakwash lake fault that is known to strike across the region from the west grid to the east grid. The fault represents the contact or suspected contact between the granitic and volcanic rocks to the north and the metasediments to the south. Both of the grids were designed to cross-cut the suspected fault location with the intent of testing the fault for anomalies that may be consistent with deposition of gold bearing materials.

The area does not offer much in the way of exposed outcroppings so potential areas of interest were not visible to enhance the grids.

Strong IP anomalies were identified on across both grids. What was the most definitive outcome was the nature of the chargeability responses. The main area of interest outlined on both grids was the chargeability negative response that was followed by a chargeability high unit. These responses would normally correlate to resistivity highs with flanking lows.

When comparing the results over the two grids it was suggested that the features may be representing two major shear zones that strike across the entire area. Shears are the main controlling structures for gold in the Red Lake mines as well as the newly discovered Great Bear Dixie Lake project directly to the north of the Golden Goliath property.

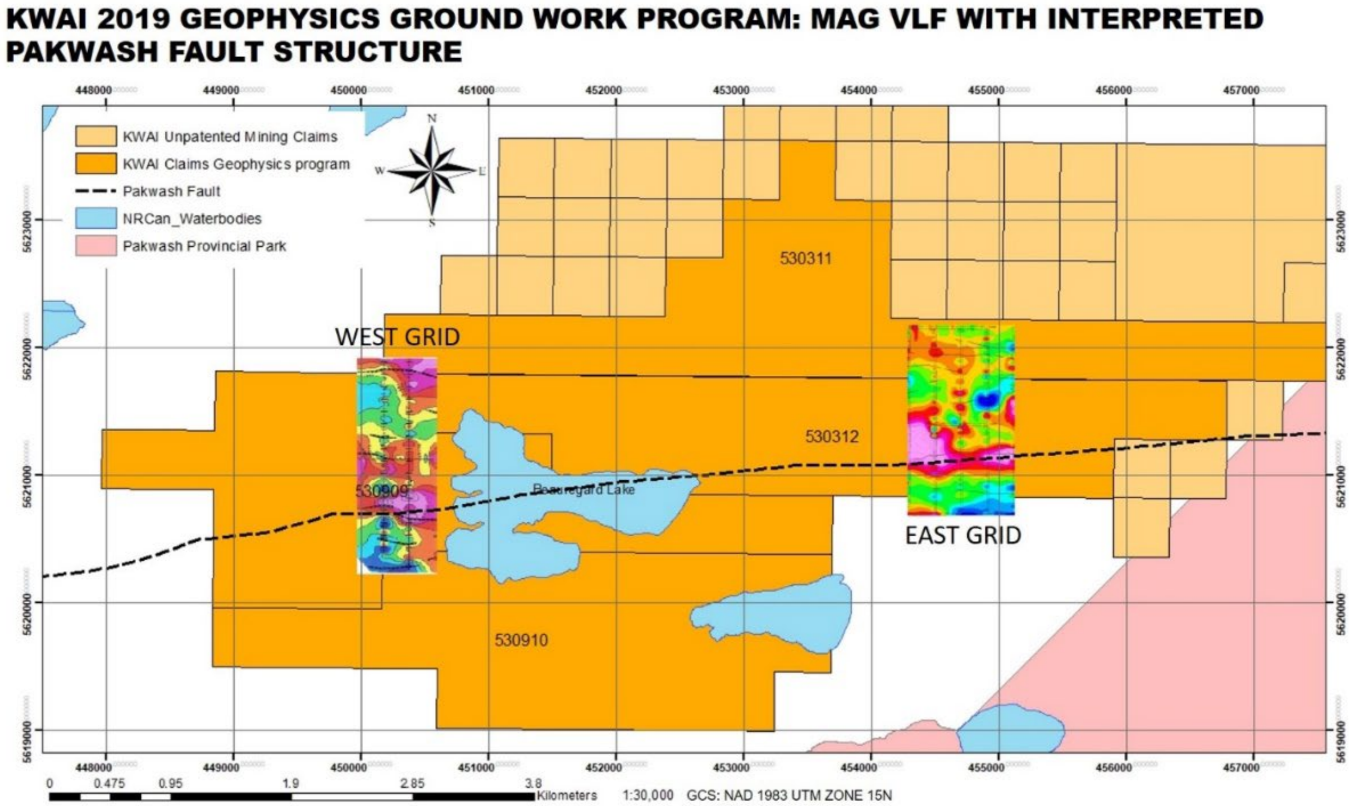

Figure 7: KWAI 2019 Geophysics Groundwork Program

REGIONAL GEOLOGY

Derived from Render et al (2011)[4].

The Kwai Property lies within the Superior Province, straddling the suture zone between the eastwest trending, Mesoarchean North Caribou and Winnipeg River Terranes to the north and south respectively. More specifically, the property is underlain by rocks assigned to the Uchi subprovince of the North Caribou terrane in the north, and the English River subprovince in the south.

[4] Render et al. (2011)

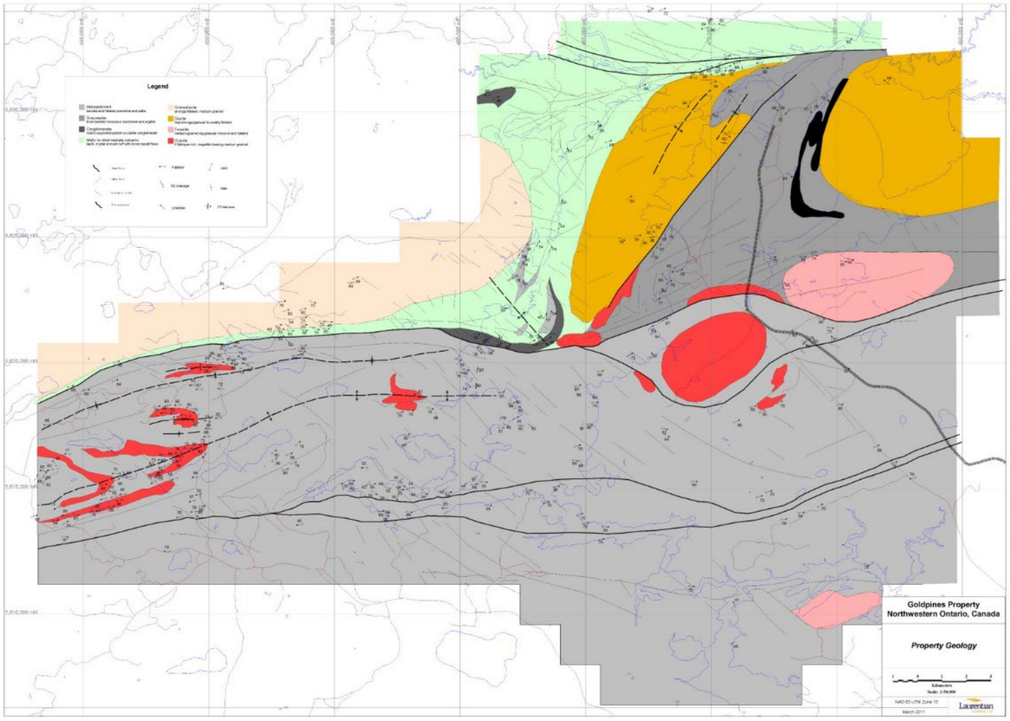

Figure 8: Laurentian Goldfields/Goldpines Interpreted Geology

The Uchi subprovince is a chain of greenstone belts characterized by strongly deformed successions of supracrustal rocks and intrusive complexes formed over protracted periods of rifting and arc magmatism. The Uchi subprovince is one of the more prolific mineral belts in the Superior Province, hosting several major deposits including the world-class Red Lake gold camp. The stratigraphy of the Uchi subprovince indicates that rifting began ca. 2.99 Ga, followed by juvenile and continental arc magmatism at 2.94-2.91, 2.90-2.89, 2.85 and 2.75-2.72 Ga (Percival, 2007). The youngest rocks in the belts are typically coarse clastic sediments that locally contain detrital zircons as young as 2.703 Ga. These strata may be facies equivalents of the marine greywacke successions of the English River subprovince to the south.[5]

Multiple regional deformation events have affected the greenstone belts in the Uchi subprovince, producing steep south-dipping composite fabrics. These are constrained by age dating as pre-2.74, 2.73, 2.72 and 2.70 Ga. Regionally, gold mineralization is found to be associated with structures formed prior to 2.712 Ga and with late-stage gold localization after 2.701 Ga.[6]

The North Caribou terrane is separated from the Winnipeg River terrane to the south by a narrow eastwest trending belt of metasedimentary rocks known as the English River subprovince. These rocks underlie the southern edge of the Kwai property. They are described regionally as migmatite and diatexite, since much of the belt has been subjected to middle amphibolite facies to low-pressure granulite facies (750-850^{0}C at 0.6-0-7 MPa) metamorphism; however original sedimentary features are

[5] Percival, J.A., 2007, Geology and metallogeny of the Superior Province, Canada, in Goodfellow, W.D., ed., Mineral Deposits of Canada: A Synthesis of Major Deposit Types, District Metallogeny, the Evolution of the Geological Provinces, and Exploration Methods; Geological Association of Canada, Mineral Deposits Division, Special Publication No. 5, p. 903-928.

[6] Percival et al. (2007)

locally preserved. The sedimentary protoliths of the English River schists and migmatites are generally immature, turbidtic greywackes. The turbidites are interpreted to be syn-orogenic flysh successions that were deposited into a forearc basin and subsequently telescoped, forming an accretionary prism at the leading edge of the Winnipeg River terrane. Detrital zircon analysis indicates that the English River sediments were deposited between 2.705 Ga and 2.698 Ga, after cessation of volcanic activity in the adjacent arc terranes. Metamorphism of the sediments has been dated at 2.691 Ga, which was followed by intrusion of 2.65 Ga volatile-rich pegmatites.[7]

Structurally, the English River subprovince is characterized by a well-developed, east-west trending composite foliation fabric defined by migmatitic layering parallel to banding in the metasediment. The fabric is folded by a tight, upright, to weakly asymmetric, north-verging F2 fold system (Hrabi and Cruden, 2001). Macroscale F1 folds are locally identified by their interference with this regional fold system.

The English River subprovince is juxtaposed against the Uchi subprovince to the north by the Sydney Lake – Lake St. Joseph fault. This east-west trending brittle-ductile fault zone is up to 3km wide and is interpreted to be subvertical to steeply south-dipping. The fault is estimated to have a dextral transcurrent displacement of about 30km and a south-side-up vertical displacement of about 2.5 km.[8] The timing of movement on the fault zone is constrained by an offset marker that is dated to 2.68 Ga.[9] (Bethune et al., 2000).

PROPERTY GEOLOGY

As derived from Render et al.[10][11]

Uchi Subprovince

Rock units assigned to the Uchi subprovince occurring in the Kwai Property include mafic to intermediate volcanic rocks and fine-grained, bedded volcaniclastic rocks. Clastic sedimentary rocks that lie north of the Pakwash Lake Fault zone are assigned to the Uchi subprovince because they are texturally different from the metasedimentary rocks of the adjacent English River subprovince to the south. These sedimentary successions are very similar in composition and may represent facies equivalents that have been juxtaposed during orogenesis.

The sedimentary unit is dominated by gritty fine-grained sandstones and greywacke (containing up to 40% mica). In the north, the unit contains a thick succession of laminated argillite and interbedded argillite and greywacke. These strata host an ironstone succession that was exploited by the past producing

Griffith Iron Mine (Figure 5). A thin unit of cobble conglomerate occurs along the trace of the Pakwash Fault. The conglomerate contains rounded clasts of diorite to granodiorite that are supported in a fine-grained,

---

7 Percival et al. (2007)

8 Stone, D., 1981, The Sydney Lake fault zone in Ontario and Manitoba, Canada. Ph.D. thesis: University of Toronto, Toronto Canada.

9 Bethune, K., Helmstaedt, H., and McNicoll, V.M., 2000, U-Pb geochronology bearing on the timing and nature of deformation along the Miniss River Fault; in Harrap, R.M., and H. Helmstaedt, H., eds., Western Superior Transect Seventh Annual Workshop: Lithopropbe Report 77, p 8-12.

10 Render, M., Meade, S.R., Lengyel, J.W.P., 2010. Goldpines North Property, Ear Falls Area, Ontario, Canada; *prepared for* Laurentian Goldfields Ltd. AFRI 20009807.

11 Render, et al. (2011)

thinly bedded, black matrix. Petrographic analysis of this unit indicates that the matrix may be volcaniclastic in origin. Interbedded volcanic and sedimentary rocks are observed locally suggesting that the two units were deposited contemporaneously. The sedimentary/volcanic succession is typically strongly foliated and contains metamorphic mineral assemblages including garnet, that are indicative of upper greenschist to lower amphibolite grade metamorphism. The supracrustal rocks are intruded by a granodiorite of undetermined age covering the majority of the north portion of the property.

English River Subprovince

Metasedimentary rocks of the English River subprovince underlie the southern part of the Kwai North property. This unit includes psammitic to pelitic rocks that are variably recrystallized, strongly foliated and banded. Mineralogically the unit is fairly homogeneous; its mineral assemblage consists dominantly of quartz and biotite with minor feldspar. Garnet commonly occurs as a porphyroblast phase indicating amphibolite facies metamorphism. The crystals range in size from 1mm to 3cm. The modal proportions of quartz and biotite are variable, which is attributed to the mud content of the original sedimentary rock. Although sedimentary layering is not preserved, compositional banding defined by biotite content occurs at the decimetre to metre-scale and is interpreted to reflect a protolith consisting of interbedded mudstone and muddy sandstone. This is consistent with regional interpretations of the English River as a flyshoid greywacke succession.

The metasediment is intruded by pegmatite dykes that are dominantly tonalitic in composition, consisting of plagioclase, quartz and biotite. Accessory phases locally noted include garnet, beryl, and tourmaline. Lesser granitic pegmatite occurs in some portions of the claim area. It contains K-feldspar, plagioclase, quartz, biotite and muscovite. The dykes range from cm-wide stringers to small plutons several metres in diameter. They are consistently parallel to the main foliation in the rock but the degree to which the dykes are transposed is variable. Throughout most of the claim area pegmatite dykes are demonstrably infolded with deformed metasediment, describing tight, weakly asymmetrical fold wave trains. In high strain zones, dykes are commonly dismembered and boudinaged with fabric in the surrounding metasediment wrapping around the deformed dyke. At some localities, highly transposed dykes form regular banding to the extent that these portions of the unit may be characterized as metatexite.

Structure

The English River and Uchi subprovinces in the Property area are separated by the Pakwash Lake Fault, a major east-west trending fault that is interpreted to splay from the Sydney Lake Fault zone, located south of the property.

The Pakwash Lake Fault is tightly constrained by mapping, but fault rocks are rarely exposed, suggesting that along much of its length it is a narrow zone of deformation. It is interpreted to be roughly parallel to the steeply south dipping foliation fabric expressed in sedimentary rocks adjacent to the fault zone.

Outcrops within the deformation zone show a combination of brittle and ductile deformation features suggesting the fault had a protracted history of movement. The fault rocks typically show well developed C-S fabrics that indicate apparent dextral shear sense. The ductile fabrics are locally overprinted by annealed, fabric-parallel brittle faults and thin horizons of fault breccia that similarly show right-lateral strike-slip movement.

AIRBORNE GEOPHYSICAL SURVEY PROGRAM

2020-03-20 to 2020-03-24

This section presents and summarizes the results of 4 field days of Airborne geophysical surveys, completed March 20- 24th , 2020; with subsequent data processing, interpretation and reporting delivered August 2020, on the Kwai property, located in the Cabin Bay and Dixie Lake Area in the Red Lake mining district. Fieldwork was completed by Pilot Nick Muller and operator David Salvatori, employed by Terraquest Ltd., under contract to Golden Goliath Resources Ltd. The Kwai Unpatented Claim land package is 100% held by EMX Properties (Canada) Inc. and all claim surface rights are currently held by the Crown.

WORK PROGRAM PURPOSE AND OBJECTIVES

Building off the recommendations of the 2019 Exploration work program, the purpose of this survey is to collect geophysical data that can be used to prospect directly for economic minerals that are characterized by anomalous magnetic or conductive responses. Secondly, the geophysical patterns can be used indirectly for exploration by mapping the geology in detail, including faults, shear zones, folding, alteration zones and other structures. The data are carefully processed and contoured to produce grid files and maps that show distinctive patterns of the magnetic and VLF Electromagnetic data to guide and further refine exploration.

WORK PROGRAM DAILY LOG

March 20, 2020:

Muller and Salvatori mobilize to operations base in Red Lake, ON (Red Lake Airport XXXX).

March 21, 2020:

Muller and Salvatori conduct calibration flight

March 22, 2020:

Crew conduct two survey flights, xxxx

March 23, 2020:

Crew initially processes data in field for quality control and accuracy

March 24, 2020:

Crew demob from Red Lake to home base

March- August 2020:

Additional data processing, interpretation and modelling work along with a final report are prepared and submitted.

Equipment Position and Specifications:

Figure 9: Survey Aircraft- Cessna U206 with sensor arrays

The primary airborne geophysical equipment includes three high sensitivity cesium vapour magnetometers and a Matrix Total Field, frequency specific VLF-EM system. Ancillary support equipment includes a tri-axial fluxgate magnetometer, radar altimeter, barometric altimeter, GPS receiver with a real-time correction service, and a navigation system. The navigation system comprises a left/right indicator for the pilot and a screen showing the survey area, planned flight lines, and the real time flight path. All data were collected and stored by the data acquisition system. For the Airborne and Base station Equipment Specifications for all the instruments and sensors used in the performance of the survey, please refer to Appendix B, Section 3.3 and 3.4 pages 10-12. The Magnetic and VLF sampling interval is 6.1m (10Hz).

WORK PROGRAM SUMMARY

To obtain this data, the area was systematically traversed by aircraft carrying geophysical equipment along parallel flight lines. The lines are oriented to intersect the geology and structure so as to provide optimum contour patterns of the geophysical data.

High resolution horizontal gradient magnetic data have provided a detailed data set which can be used to improve the magnetic mapping. The Matrix VLF-EM total field products show good correlation with both magnetic and geologic trends and have been successful in identifying and mapping the structural fabric across the survey area. The Matrix VLF-EM data have been inverted to obtain resistivity data channels, grids and map images of depth slices of the inverted VLF-EM, plus voxels to enable 3D viewing of the VLF-EM Resistivity interpretation.

WORK PROGRAM RECOMMENDATIONS

1. A program of geological mapping at 1:10000 scale to better tie the geophysics into the property geology.
2. Ground geophysics using induced polarization to identify areas of chargeability associated with the structures shown on the VLF.
3. Diamond drilling program to test priority targets.

STATEMENT OF QUALIFICATIONS

I, Gordon C. MacKay, of 299 Birch Street, Lively Ontario hereby certify that:

1. I am the author of this report.

2. I graduated from the University of British Columbia, in Vancouver, with a Bachelor of Science Degree in Geology (1988).

3. I possess an Ontario prospector's license and have been practising my profession in mineral exploration industry for the past 34 years.

4. I am a practicing member of the Association of Professional Geoscientists of Ontario.

Sudbury, Ontario
March 10, 2022

Gordon C. MacKay P. Geo.
MacKay Mining Solutions

OPERATIONS REPORT

For

Golden Goliath
RESOURCES LTD

Horizontal Magnetic Gradient &
Matrix VLF-EM-Resistivity
Airborne Survey

Kwai Property
Red Lake, ON

File: B503

August 18, 2020

Requested by
Bob Middleton
Consulting Geophysicist
Golden Goliath Resources

Prepared by:
Charles Barrie, M.Sc., P.Geo
VP/Owner
Terraquest Ltd.

Table of Contents

1. INTRODUCTON

1.1. EXECUTIVE SUMMARY

This report describes the specifications and parameters of an airborne geophysical survey carried out for:

GOLDEN GOLIATH RESOURCES
Suite 910 – 688 West Hastings Street
Vancouver, BC
V6B 1P1

Attention: Paul Sorbara, CEO
Email: jps@goldengoliath.com

The survey was performed by:

TERRAQUEST LTD.,
301-2900 John Street
Markham ON, Canada
L3R 5G3

Phone: 905-477-2800 ext. 31
Email: cb@terraquest.ca.

The purpose of this survey is to collect geophysical data that can be used to prospect directly for economic minerals that are characterized by anomalous magnetic or conductive responses. Secondly, the geophysical patterns can be used indirectly for exploration by mapping the geology in detail, including faults, shear zones, folding, alteration zones and other structures. The data are carefully processed and contoured to produce grid files and maps that show distinctive patterns of the magnetic and VLF Electromagnetic data to guide and further refine exploration.

To obtain this data, the area was systematically traversed by aircraft carrying geophysical equipment along parallel flight lines. The lines are oriented to intersect the geology and structure so as to provide optimum contour patterns of the geophysical data.

1.2. LOCATION

The Red Lake Project is located approximately 430 kilometres northwest of Thunder Bay, Ontario, in the Dixie Lake and Cabin Bay Areas of the Red Lake Mining Division, Ontario, and approximately 30 kilometres south of the town of Red Lake, 34 kilometres northwest of the town of Ear Falls and 5 kilometres west of Pakwash Lake. The property can be readily accessed by from the TransCanada Highway to Highway 105 to the Dixie Lake road.

The survey area is irregular and generally elongate in shape with 15 corners. The main dimensions are approximately 10 kilometres east-west dimension and 3.3 kilometres north-south. The centre of the survey is approximately 50°44'30" N and 93°11'40" W.

Regional Location

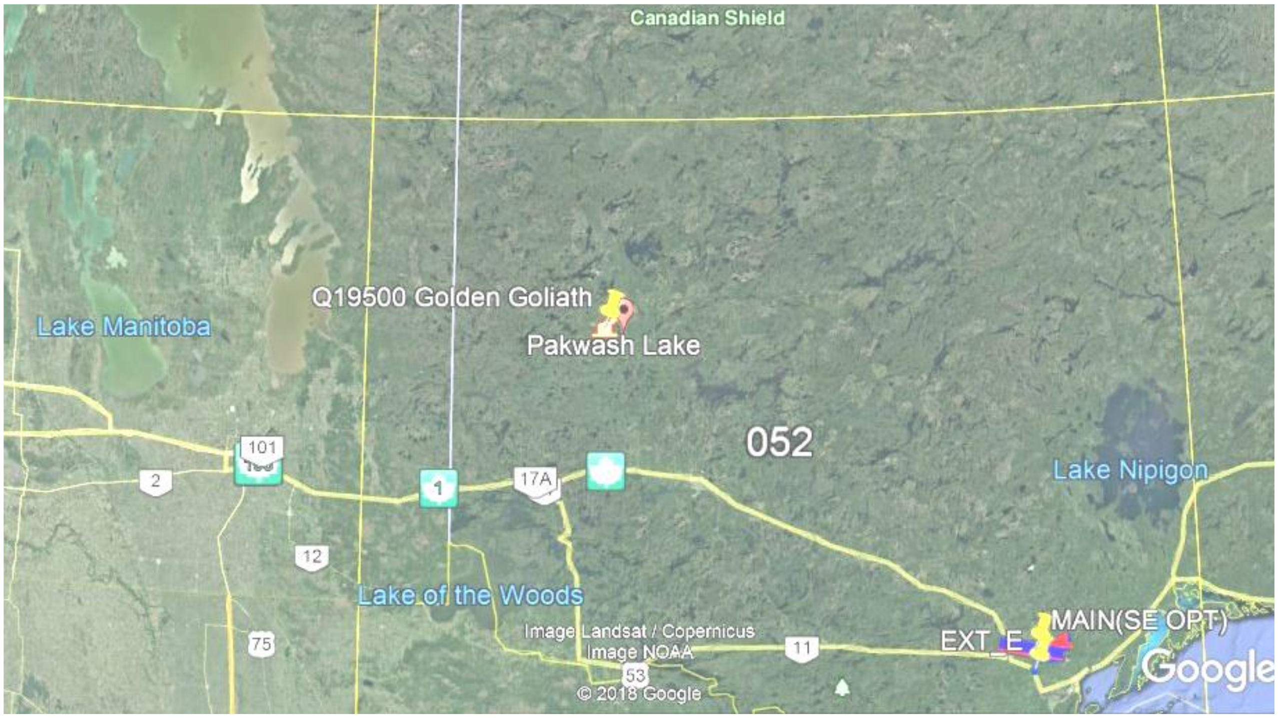

Detail Location

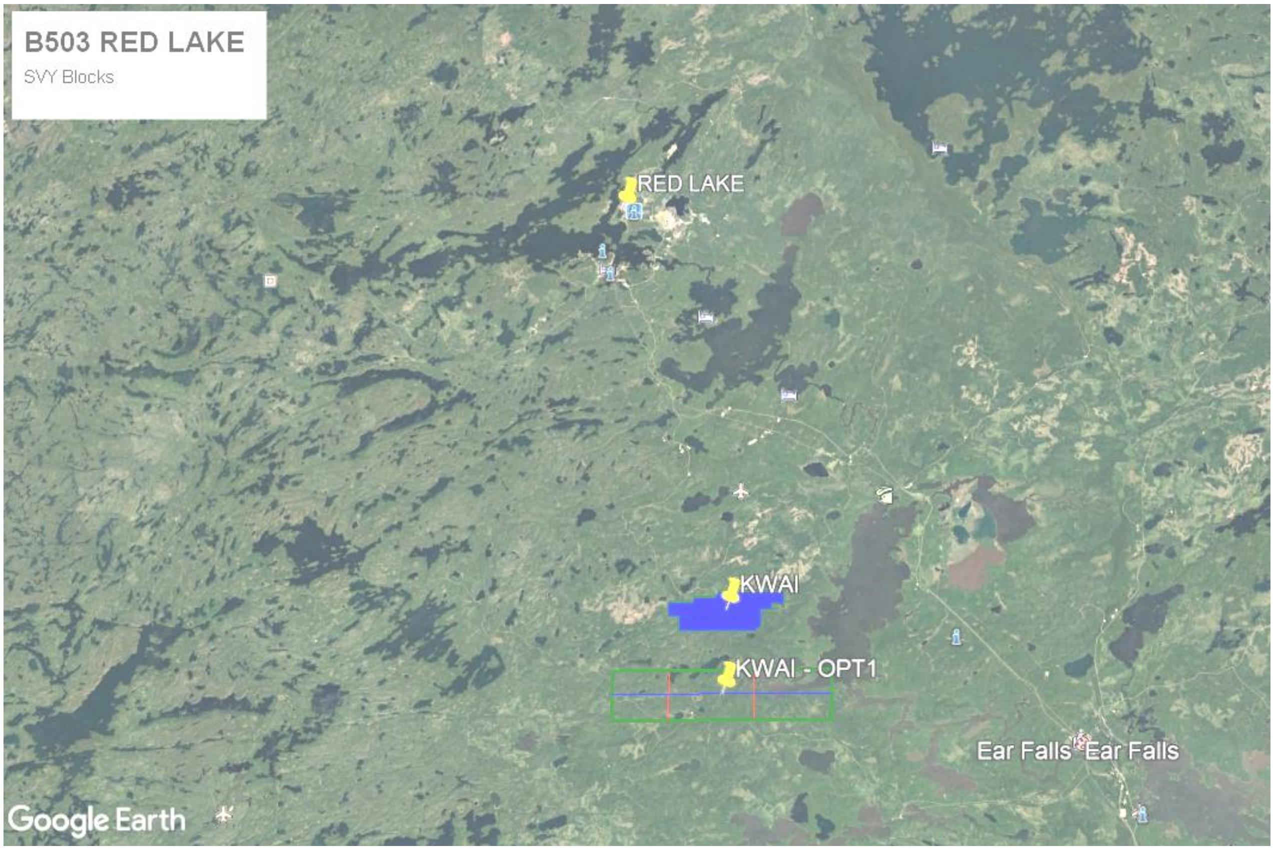

2. SURVEY SPECIFICATIONS

2.1. LINES AND DATA

Parameter	Specification
Aircraft Speed	mean 61.3 m/sec 220.7 km/hr
Magnetic & VLF Sampling Interval	6.1 m (10Hz)
Flight-line Interval	100 metres
Flight-line Direction	000/180 degrees
Control-line Interval	900 metres
Control-line Direction	090/270 degrees
Mean Terrain Clearance	59.6 metres

2.2. SURVEY KILOMETRAGE

B503: RED LAKE PROJECT					
LINE		TIE		Total	
NLIN	KM	NLIN	KM	NLIN	KM
100	246.6	4	30.5	104	277.0

2.3. NAVIGATION SPECIFICATIONS

The satellite navigation system was used to ferry to the survey and to survey along each line. The survey coordinates were supplied by the client and were used to establish the survey boundaries and flight lines. The flight path guidance accuracy is variable depending upon the number and condition (health) of the satellites employed. With WAAS real time correction the accuracy was for the most part better than 3 metres.

The following are the navigation files used for the Red Lake Project, B503. These files include survey corner coordinates in WGS84 projection Zone 15N, line spacing, line direction, master line and other navigational parameters:

```
0  KWAI
1  Z 15
2      448780     5619460       AREA CORNER 1
2      448800     5620730       AREA CORNER 2
2      447950     5620745       AREA CORNER 3
2      447965     5621840       AREA CORNER 4
2      450158     5621840       AREA CORNER 5
2      450153     5622271       AREA CORNER 6
2      452093     5622255       AREA CORNER 7
2      452400     5622770       AREA CORNER 8
2      457910     5622700       AREA CORNER 9
2      457915     5621705       AREA CORNER 10
2      456813     5621710       AREA CORNER 11
2      456800     5621250       AREA CORNER 12
2      455930     5621250       AREA CORNER 13
2      455910     5619880       AREA CORNER 14
2      455470     5619400       AREA CORNER 15
3      448780     5619460     W WAYPOINT 1
3      448780     5619460  COR1 WAYPOINT 2
```

```
4          100                 NUMBER OF LINES
5        100.0                 SPACING, m
8           75                 MAX CROSS TRACK, m
9    0  0  0                   DELTA X/Y/Z
10           1                 LOG FPR EVERY 1 SECS
11 0.9996000000       0.0      0.0 K0, X/Y SHIFT
14           0                 LINES EXTENDED BEYOND AREA
16          10                 FIRST LINE NUMBER
17   447975.0   5620755.0   0.0 MASTER POINT, HEADING
18   456780.0   5625350.0  90.0 TIE LINE MASTER POINT, HEADING
19      900.0          0       TIE LINE SPACING, LINE EXTENSION, m
20 WGS-84      6378137.0   298.257223563 22       ELLIPSOID
21           0                 NO EQUATORIAL CROSSING, N HEMISPHERE
30          20    9600  N  1  8  RS-232 PORT 2 INCOMING FORMAT
31          20    9600  N  1  8  RS-232 PORT OUTGOING FORMAT
38           0                 METRIC SYSTEM
41        0.00                 SYSTEM LAG, Secs.
80         0.00                PLANNED ALTITUDE, m
83           0                 GPS ALTITUDE FOR VERTICAL BAR
84        0.00       0.00      ALTITUDE COEFFICIENT, OFFSET
85         100                 MAX VERTICAL BAR SCALE
102  UTM                       UTM X/Y SCALE
```

Navigation Plot

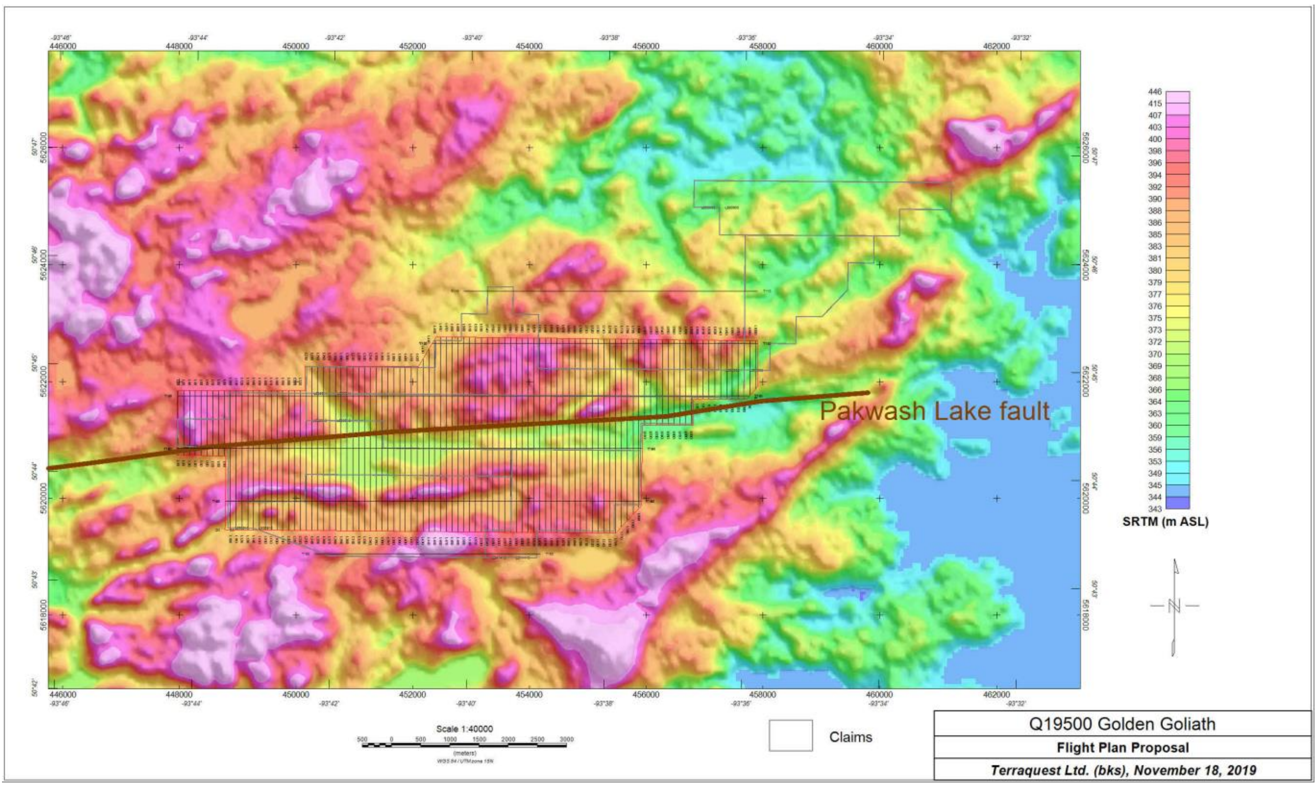

2.4. TOLERANCES - REFLIGHT

1. Traverse Line Interval

Re-flights would take place if the cross-track deviation of the final differentially corrected flight path from the preplanned flight path is greater than 25 metres over a distance greater than 1 kilometre.

2. Terrain Clearance:

The contract called for a terrain clearance of 50-70 metres where safely possible. A computer-generated drape surface was made to guide the terrain clearance, setting the target clearance of 60 metres but it was not used because at this low terrain clearance, it often acts as a distraction; consequently terrain clearance was determined by standard visual and radar altimeter procedures. The mean survey terrain clearance was 59.6 metres.

3. Diurnal Variation:

Diurnal activity during survey data acquisition was limited to less than 3 nT non-linear deviations from a 1-minute chord.

4. GPS Data:

GPS data included at least 4 satellites for navigation and flight path recovery. There were no significant gaps in any of the digital data including GPS and magnetic data.

5. Radio Transmission:

The aircraft pilot makes no radio transmission that interferes with magnetic responses.

6. Sample Interval:

A reflight is required if the sample interval along one or more of the survey lines exceeds 10 metres over a cumulative total of 1000 metres.

3. AIRBORNE GEOPHYSICAL EQUIPMENT

3.1. SURVEY AIRCRAFT

The Cessna U206, registration C-GGLS, owned and operated by Terraquest Ltd. was the survey aircraft for the Kwai Project. This aircraft is approved by the Canadian Ministry of transport and has a certification for specialty flying that includes airborne geophysical surveys. This aircraft is maintained by a regulatory AMO facility, Enterprise Air Ltd. in Oshawa, ON.

The aircraft has been specifically modified with long-range fuel cells to provide up to 7 hours of range, outboard tanks, tundra tires, cargo door, and avionics as well as an array of sensors to carry out airborne geophysical surveys.

3.2. AIRBORNE EQUIPMENT OVERVIEW

The primary airborne geophysical equipment includes three high sensitivity cesium vapour magnetometers and a Matrix Total Field, frequency specific VLF-EM system. Ancillary support equipment includes a tri-axial fluxgate magnetometer, radar altimeter, barometric altimeter, GPS receiver with a real-time correction service, and a navigation system. The navigation system comprises a left/right indicator for the pilot and a screen showing the survey area, planned flight lines, and the real time flight path. All data were collected and stored by the data acquisition system. The following is a summary of the equipment specifications:

Aircraft	Cessna U206 / C-GGLS
Equipment:	
Magnetometers	Scintrex CS-2&3 Cesium Vapour
3-axis Fluxgate Magnetometer	Billingsley TFM100-LN
VLF-EM (proprietary)	Magenta Matrix Frequency Specific VLF-EM

GPS Receiver	Hemisphere R230 with WAAS real time Atlas correction
Radar Altimeter	King KRA 10A
Barometric Altimeter	Sensym LX18001AN
Acquisition	RMS Instruments DAARC 500
Navigation	AgNav Inc. P151 Linav system
Magnetic Configuration & Specifications:	
Lateral Sensor separation	13.21 metres
Longitudinal Sensor separation	8.87 metres
FOM	<1.5 nT
Sensitivity	0.001 nT

The 13.75 volts aircraft power is converted to 27.5 volts DC for the geophysical equipment by an ABS power supply.

3.3. AIRBORNE EQUIPMENT SPECIFICATIONS

1. Magnetics:

Three high-resolution cesium vapour magnetometers, manufactured by Scintrex, were installed in the tail stinger and two wing tips extensions; the transverse separation was 13.21 metres and the longitudinal separation was 8.87 metres.

Cesium Vapour Magnetometer	(mounted in tail stinger and wing tip extensions)
Manufacturer	Scintrex
Models	CS-2, CS-3
Resolution	0.001 nT counting at 0.1 per second
Sensitivity	+/- 0.005 nT
Dynamic Range	15,000 to 100,000 nT
Fourth Difference	0.02 nT

2. Data Acquisition & Magnetic Compensation System

DAS & Compensation	Combined; real time compensation
Model	DAARC 500
Manufacturer	RMS Instruments
Operating System	QNX 6.3 or greater
Time	104 MHz temperature compensated crystal clock
Front End Magnetic Processing	Resolution 0.32pT; system noise <0.1pT; sample rate 160, 640, 800m or 1280 Hz
Front End - Fluxgate	I/F module; oversampling, self-calibrating 16 bit A/D converter
Compensation	Improvement Ratio (total field) 10-20 typical
Input Serial	8 isolated RS232 channels; ASCII & Binary formats
Input Analog	16 bit, self-calibrating A/D conv.
Input Events	Four latched event inputs
Raw Data Logging	At front end sampling rate, 1 MB buffer
Output/Recording	Rate 10, 20 or 40 Hz; Serial up to 115.2 kbps; Recording media 1 GB Flash; 80 GB Hard Drive; Flash disk via USB; Display
Front Panel Indicators	8 LEDs for mag input; 2 LEDs for Front End status

3. Navigation System

Navigation System	
Model	P151
Manufacturer	AgNav Inc.
Operating System	Linex
Microprocessor	CPU Pentium based
Ports	RS232 for all devices
Graphic Display	Colour Screen
Pilot Display	P202: position, left/right, navigational info

4. Real-Time Correction GPS Receiver

GPS Differential Receiver	
Model	R120
Manufacturer	Hemisphere
Output	NMEA string, PPS
Channels	12 Channel DGPS, internal L-band
Position Update	0.5 second for navigation
Correction Service	Real time correction service WAAS
Sample Rate	Up to 10hz, set at 5 hz

5. Magenta Digital, Frequency Specific VLF-EM System

The Matrix VLF-EM System by Magenta is a newly developed digital, frequency specific VLF-EM system. The sensor consists of 3 orthogonal coils mounted in the tail stinger which are coupled with a receiver-console. The Matrix VLF-EM System measures the total field strength (amplitude - the vector sum of all coils). The data are recorded on three VLF frequencies: Cutler Maine NAA frequency 24.0 kHz, La Moure North Dakota NML frequency 25.2 kHz and Seattle, WA NLK frequency 24.8 kHz, which yield outputs of Total Field, Vertical and Planar Ellipticities, azimuth to transmitter and Tilt Angle.

VLF – EM	Source field
Model	Matrix
Manufacturer	Magenta Ltd.
Primary Source	Magnetic field component radiated from government VLF radio transmitters
Output Parameters	Total Field Strength, Vertical and Planar Ellipticities, Azimuth to Transmitter and Tilt Angle
Frequency Range	Cutler (24.0 kHz), La Moure (25.2 kHz) and Seattle (24.8 kHz)
Gain	Constant gain setting
Filtering	No filtering

6. Tri-Axial Fluxgate Magnetic Sensor

The fluxgate tri-axial magnetometer was mounted in the rear of the aircraft cabin to monitor aircraft manoeuver and magnetic interference. This was used to compensate the high sensitivity data in real time.

Tri-Axial Fluxgate Magnetic Sensor	(for compensation, mounted in mid-section of tail stinger)
Model	TFM100-LN
Manufacturer	Billingsley Magnetics
Description	Low noise miniature triaxial fluxgate magnetometer
Axial Alignment	> Orthogonality > +/- 0.5 degree

Accuracy	< +/- 0.75% of full scale (0.5% typical)
Field Measurement	+/- 100,000 nanotesla
Linearity	< +/- 0.0035% of full scale
Sensitivity	100 microvolt/nanotesla
Noise	< 14 picotesla RMS/–Hz @ 1 Hz

7. Radar Altimeter

Radar Altimeter	
Model	KRA-10A
Manufacturer	King
Serial Number	071-1114-00
Accuracy	5% up to 2,500 feet
Calibrate Accuracy	1%
Output	Analog for pilot, converted to digital for data acquisition

8. Barometric Altimeter

Barometric Altimeter	
Model	LX18001AN
Manufacturer	Sensym Inc.
Source	Coupled to aircraft barometric system

3.4. BASE STATION EQUIPMENT

The magnetometer was the same type used in the aircraft, a cesium magnetometer manufactured by Scintrex. The magnetometer processor was a KMAG manufactured by Kroum VS Instruments and the data logger was a PDA by Archer. The counter was powered by a 10VAC 50/60 Hz to 30VDC 3.0-amp power supply with an internal 12VDC fan. The logging software SDAS-1 was written by Kroum VS Instrument Ltd. specifically for handheld pc hardware. It supports real time graphics with selectable windows (uses two user selectable scales, coarse and fine). Time recorded was taken from the base GPS receiver. Magnetic data was logged at 1Hz. Data collection was by RS232 recording ASCII string and stored on flash card.

Magnetometer Type	Cesium Vapour
Model	CS-3
Manufacturer	Scintrex Ltd.
Sensitivity	0.022 nT / vHz@1Hz
Resolution	0.001 nT
Dynamic Range	15,000 – 120,000 nT
GPS model	GPS 18
GPS manufacturer	Garmin

4. TESTS AND CALIBRATIONS

4.1. MAGNETIC FIGURE OF MERIT

Compensation calibration tests were performed to determine the magnetic influence of aircraft maneuvers and the effectiveness of the aircraft compensation method. The aircraft flew a square pattern in the four survey directions at a high altitude over a magnetically quiet area and performed pitches (± 5°), rolls (± 10°) and yaws (± 5°). The sum of the maximum peak-to-peak residual noise amplitudes in the total compensated signal resulting from the twelve maneuvers is referred to as the FOM. The FOM was flown on March 22, 2020, Flight 1979 and the values for this survey were 1.22 nT, 1.64 nT and 0.66 nT for the Left, Right and Tail sensors respectively (see Appendix II).

4.2. MAGNETIC LAG

Evaluation of the magnetic lag factor was accomplished by comparing survey data flown over a series of distinct magnetic anomalies in opposing directions. The measured lag was 0.5 seconds for the wingtip sensors and 0.70 seconds for the tail sensor. The results are presented in the following table:

C-GGLS : LAG EVALUATION
Flown: 13 September, 2019 (Flight GLS1864)

WINGTIP SENSORS (TF1, TF2)

LINE	DIR		Reference Anomaly							
			A	B	C	D	E	F		
L3502:1864	135°	FIDUCIAL	74879.9	74866.9	74850.3	74826.9	74817.4	74794.3		
		X	300990.6	300483.4	299803.4	298835.3	298448.9	297521.7		
		Y	4854472.2	4854973.9	4855654.5	4856628.2	4857009.2	4857946.3		
		SPEED (S_1)	54.6	55.8	58.7	58.1	57.1	57.3		
L3503:1864	315°	FIDUCIAL	74996.9	75008.3	75023.8	75046.1	75055.1	75077.5		
		X	300951.4	300448.4	299759.3	298793.2	298413.3	297487.4		
		Y	4854515.4	4855016.2	4855702.1	4856668.9	4857053.4	4857978.3		
		SPEED (S_2)	62.8	62.3	62.1	60.3	59.3	57.4		
		DELTA (apparent directional seperation, metres)	**58.3**	**54.9**	**64.8**	**58.5**	**56.8**	**46.9**		
		LAG (secs) *	**0.5**	**0.5**	**0.5**	**0.5**	**0.5**	**0.4**	**AVG LAG**	**0.5**

TAIL SENSOR (TF3)

LINE	DIR		Reference Anomaly							
			A	B	C	D	E	F		
L3502:1864	135°	FIDUCIAL	74880.1	74867.1	74850.5	74827.1	74817.6	74794.5		
		X	300998.6	300491.2	299811.7	298843.5	298457.1	297529.8		
		Y	4854464.8	4854965.9	4855646.2	4856620.0	4857001.3	4857938.3		
		SPEED (S_1)	54.7	55.8	58.7	58.2	57.1	57.3		
L3503:1864	315°	FIDUCIAL	74997.0	75008.4	75023.9	75046.3	75055.4	75077.7		
		X	300946.8	300444.0	299755.0	298784.7	298400.7	297479.4		
		Y	4854519.7	4855020.6	4855706.5	4856677.5	4857066.0	4857986.5		
		SPEED (S_2)	62.8	62.3	62.1	60.3	59.3	57.4		
		DELTA (apparent directional seperation, metres)	**75.5**	**72.3**	**82.8**	**82.2**	**85.9**	**69.8**		
		LAG (secs) *	**0.6**	**0.6**	**0.7**	**0.7**	**0.7**	**0.6**	**AVG LAG**	**0.7**

** Lag factor calculated as LAG = DELTA/(S1+S2)*

4.3. RADAR CALIBRATION

C-GGLS: RADAR CALIBRATION DATA SUMMARY
Calibration performed: 15 Feb 2020, GLS1946

					INTERCEPT	-3.2098
					SLOPE	69.9216

LINE	RAW RADAR	GPS ALT	CORRECTED GPS ALT	LASER	CALIBRATED RADAR	ERROR *
Ground Ref		328.7	0.0			
S020	0.3754	351.1	22.4	25.3	23.0	0.6
S050	0.7966	381.1	52.4	55.1	52.5	0.1
S075	1.1464	406.2	77.5	79.8	76.9	-0.6
S100	1.5685	435.3	106.6	108.7	106.5	-0.1
S135	1.9883	464.4	135.7	138.4	135.8	0.1
S140	2.0688	470.6	141.9	140.1	141.4	-0.5
S165	2.4020	493.7	165.0	167.6	164.7	-0.3
S190	2.7268	516.5	187.8	190.7	187.5	-0.3
S215	3.1080	541.9	213.2	215.7	214.1	0.9

** Error estimated as (Calibrated Radar) - (Corrected GPS Alt)*

Imperial Units

LINE	GPS_ALT (ft)	CAL_RAD (ft)
S020	73.5	75.6
S050	171.9	172.2
S075	254.3	252.5
S100	349.7	349.3
S135	445.2	445.6
S140	465.6	464.1
S165	541.3	540.5
S190	616.1	615.0
S215	699.5	702.4

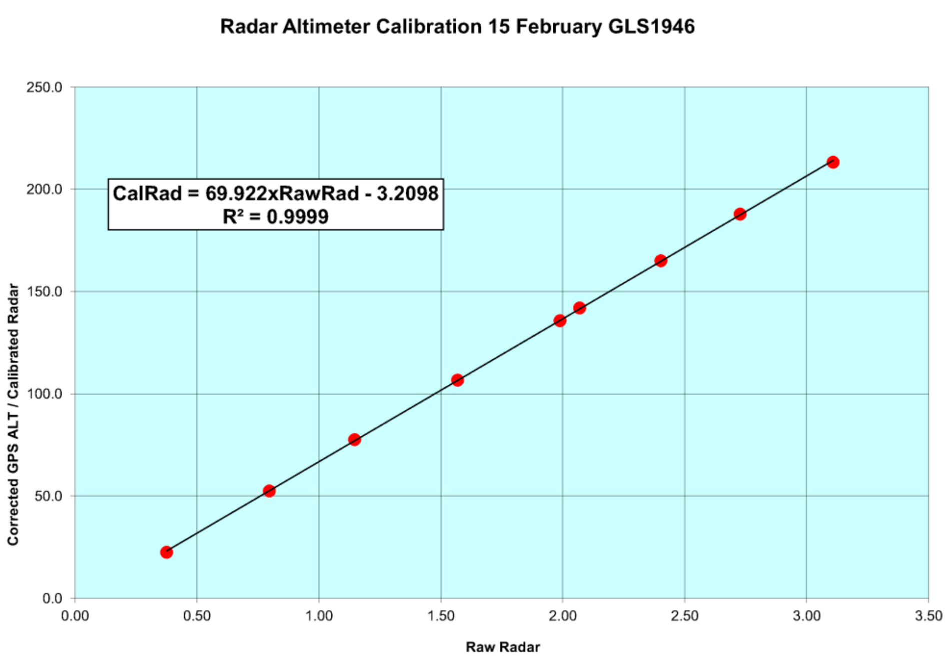

5. LOGISTICS

5.1. PERSONNEL

The contractor supplied the following properly qualified and experienced personnel to carry out the survey and to reduce, compile and report on the data:

Survey:	Pilot	Nick Muller
	Operator	David Salvatori
	Office QC Processor	Allen Duffy
	Office Final Processing	Allen Duffy
	Manager	Charles Barrie

5.2. FLIGHT REPORTING

The local Figure of Merit (FOM) calibration was flown on March 21, 2020, Flight #1979 near Red Lake at a location with a low magnetic gradient; the data were examined and a clean FOM was calculated.

The survey was flown in 2 flights (1980-1981) over 1 day on Sunday March 22nd. The traverse lines were flown on the first flight and the tie lines on the second flight. The weather was clear and no equipment or aircraft maintenance were required during the survey. The government VLF-EM transmitters were all operational. The survey data were reviewed and declared satisfactory on March 23rd, 2020. The preliminary flight path and Total Magnetic field were forwarded to the client on March 23rd and a suite of gradient magnetic and VLF-EM plots on March 24th.

During the survey, the pilot maintained daily personal, aircraft and preflight safety reports. The base station and airborne data were monitored throughout the survey and recorded by precise notes of each flight. At the end of the flight day the flight report and data were uploaded to the project geophysicist who performed quality control on the raw and compensated survey data. Additionally, the geophysicist transcribed the operator notes and entered quality control notes into a spreadsheet in excel.

All survey personnel crew adopted and worked under the Terraquest Ltd. Health, Safety and Environmental Protection Manual (which include Site Specific Safety Plan and Emergency Response Plan) along with guidelines from the IAGSA safety and security standards.

5.3. BASE OF OPERATIONS

The Terraquest base of operations was at Red Lake Airport (CYRL). The base station (combined high sensitivity magnetic and GPS) was set up at a secure location at the airport.

The crew's accommodations were the responsibility and cost of Terraquest. The crew stayed at the Howey Bay Motel, 26 Highway 105, Red Lake, ON P0V 2M0; tel: 877-464-6939. Internet was satisfactory.

6. DATA PROCESSING

6.1. DATA QUALITY CONTROL / PRELIMINARY PLOTS

The field data were examined in the evening after the two flights by a geophysicist to inspect the data for quality control and tolerances. All data were approved and checked for continuity and integrity. Magnetic data were corrected for diurnal to produce preliminary plots. The Preliminary plots of flight path and Total Magnetic field were forwarded to the client the following day on March 23rd. Preliminary plots of Flight path on DTM, Analytic Magnetic Signal, East-West Horizontal Magnetic Gradient, North-South Magnetic Gradient, Reconstructed Magnetic Field, Calculated Vertical Magnetic Field, Cutler VLF-EM, La Moure VLF-EM and Seattle VLF-EM were forwarded to the client on March 24th.

6.2. DIGITAL TERRAIN MODEL

The radar altimeter data were subtracted from the GPS altitude to produce a Digital Terrain Model (DTM). The resulting data were micro-leveled to remove line-to-line imperfections in the data. The final grids were created using bi-directional Akima spline interpolation at a cell size of 25 metres.

6.3. FINAL MAGNETIC DATA PROCESSING

1. Lag Correction of Total Magnetic Field

The evaluation of the magnetic lag factor was accomplished by acquiring survey data flown in opposite directions over a series of distinct magnetic anomalies. The measured factors were 0.7 seconds for the tail Mag and 0.5 seconds for the wing tips.

2. Diurnal Data and Diurnal Corrections of the Total Magnetic Field

Magnetic data from the Diurnal Base Station were scrutinized for spurious readings (data spikes) and any obvious cultural interference. Any such features were manually removed and the data re-interpolated (Akima spline) to maintain a continuous record. A low-pass filter (60 fid cut-off wavelength) was applied to the edited diurnal record. The resulting data was used to pre-level (diurnally correct) the measured TMI data for the Tie lines prior to implementing Tie-Traverse intersection leveling. Traverse line data were not pre-leveled with Diurnal Base Station to avoid the risk of contaminating the airborne data with any remaining imperfections in the base station record.

3. Total Magnetic Field Tie-Traverse Line Intersection Levelling

The lag corrected, pre-treated (altitude correction) data were refined using tie-line levelling. Using the Geosoft Oasis implementation of this procedure, an initial table of tie-traverse line intersection differences is compiled (together with supporting ancillary parameters such as local gradient, etc.) and intersection data is loaded into the processing databases. In a series of iterative levelling passes, outlier intersection values are either disabled or modified to refine and finalize the overall result.

4. The Magnetic Field Micro-Levelling

Minor levelling imperfections may still exist in the gradient enhanced intersection levelled data, most likely due to incomplete removal of diurnal influences in sections of lines between intersection points. These errors are removed by application of mild micro-levelling procedure whereby highly directional filtering identifies and removes residual noise correlated with the line direction. The resulting corrections are limited to the maximum amplitude of +/- 8 nT to avoid "damaging" valid, geologic responses to achieve the *Total Magnetic Intensity*.

To achieve the *Anomalous Total Magnetic Intensity* for the Kwai Block the International Geomagnetic Reference Field (IGRF) was calculated from the 2015 model year and extrapolated to 22 March 2020 at the effective mean survey elevation of 450 metres above Geoid and removed from the corrected values.

5. Calculated Vertical Derivative

The first *Vertical Derivative* was calculated using a 2D FFT operator on the Total Field data grid. Unwanted, high frequency "ringing" in the resulting 1VD grid was minimized by concurrent application of an 8th order Butterworth low pass filter with a cut-off keyed to the line spacing.

6. Analytic Signal

The Calculated *Analytic Signal*, which is derived from the three orthogonal magnetic gradients, has the advantage of producing body centric anomalies - regardless of magnetic inclination - with source edges mapped out by the function's maxima. Additionally, approximate source depth may be estimated by measuring individual anomaly widths at half amplitude.

7. Horizontal Gradients

Terraquest solves the spatial mathematical relationship of the three total field measurements (left, right and tail) by using the accurate location of the three magnetic sensors in space to directly calculate the East-West and North-South gradients, referenced to geographic north, at each point along the survey line.

Both *Horizontal Gradients* were then median-leveled to remove bias; followed by mild micro-leveling to remove any remaining imperfections. Following this, the transverse and longitudinal gradients were gridded using a bi-directional Akima algorithm and a cell size of 25 metres. The measured transverse and longitudinal gradients provide an improved rendition of the shorter wavelengths in magnetic field than the residual magnetic field measured by the tail sensor alone. This is because the direction and amplitude of the field's total horizontal gradient can be determined using the 2 measured gradients, providing information regarding the behavior of the magnetic field in-between traverse lines. Thus, it is useful to incorporate the gradient data in the preparation of the residual magnetic field grid

8. Reconstructed Total Field (RTF)

Data grids of the measured horizontal gradients were used to generate the *Reconstructed Total Magnetic Field* using the 2D FFT process described by J. B. Nelson (Nelson, 1994)*. This product (RTF) has the advantage of being un-affected by magnetic diurnal activity and excellent representation of the near surface responses, though longer magnetic spatial wavelengths are not represented due to measurement resolution limitations in the magnetometers. The resulting data units (expressed as pseudo nanoTesla) are not true nT; approximate conversion to true nT may be accomplished by application of scaling factor if required. Using the calculated Reconstructed Total Field data grid, an "RTF" Geosoft database channel is created by performing a grid look-up ("grid sample") for each data point in the production database.

** Reference: Nelson, J.B., 1994, Leveling total-field aeromagnetic data with measured horizontal gradients: Geophysics, 59, 1166-1170*

9. Grids

Magnetic data grids were created using bi-directional data interpolation (Akima) at a cell size of 25 metres.

6.4. MAGNETIC DATA MAPS

1. Flight Path on Digital Terrain Model

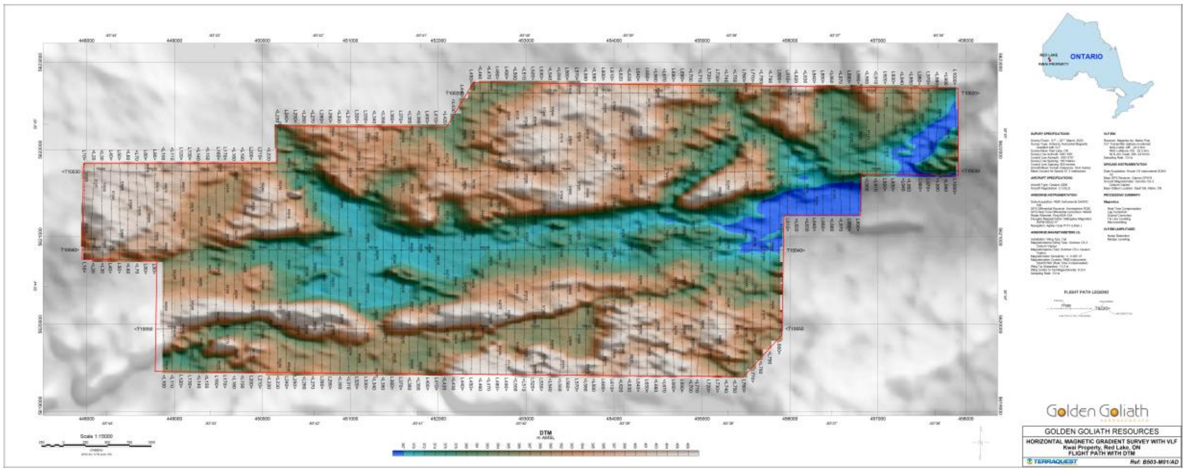

2. Total Magnetic Intensity

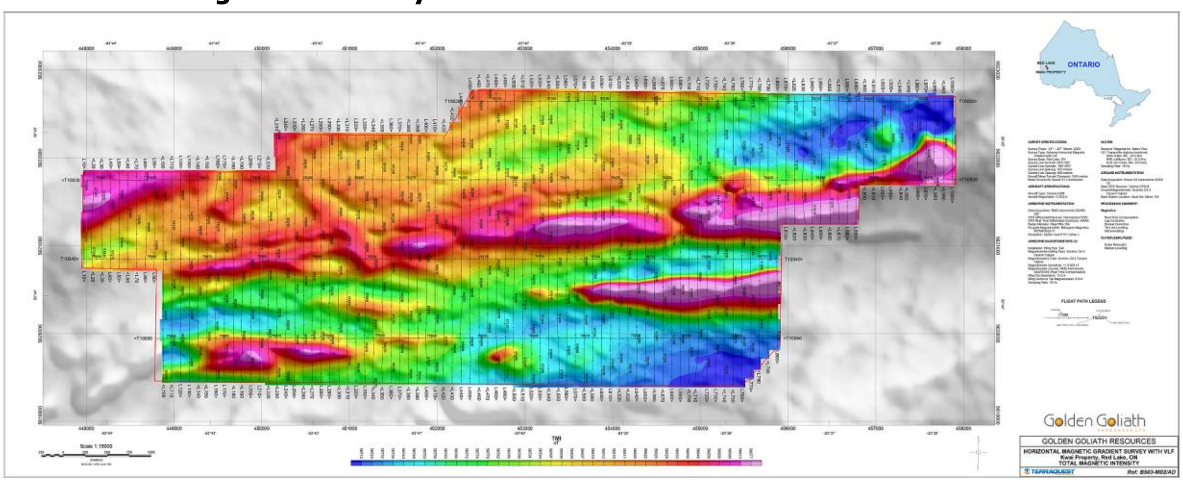

3. Anomalous (IGRF Corrected) Total Magnetic Field

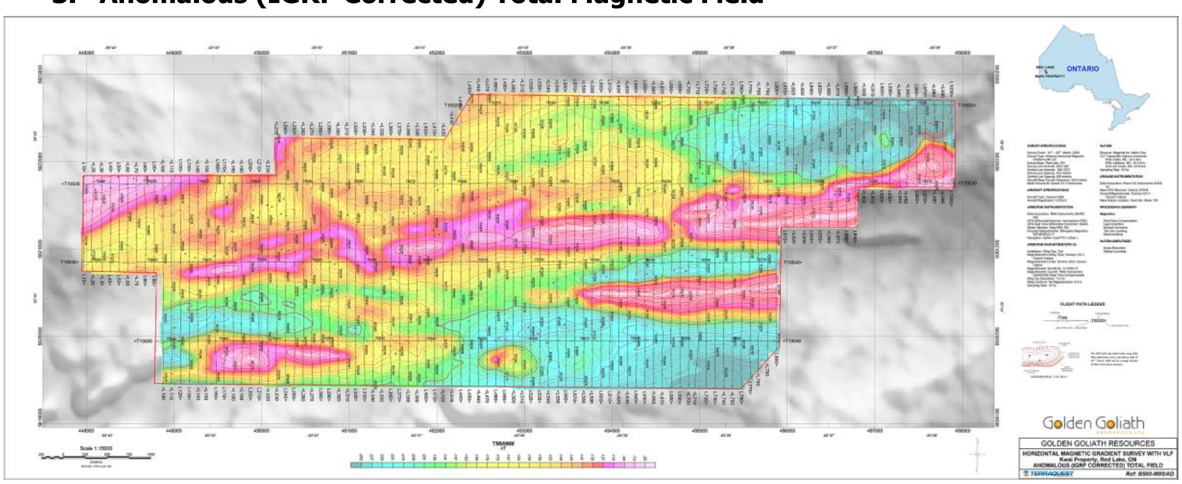

4. Calculated Vertical Magnetic Derivative

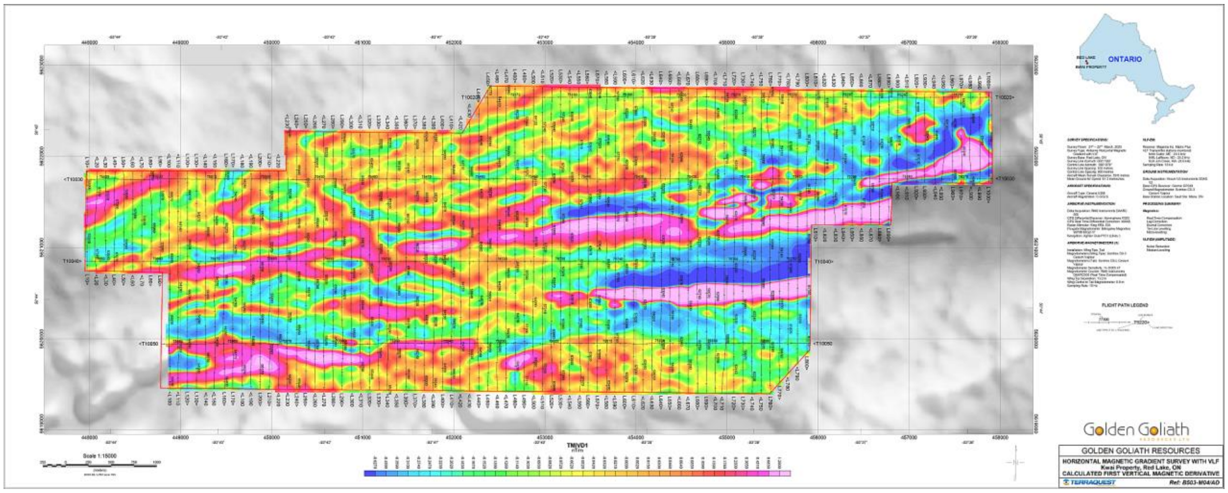

5. Analytic Signal

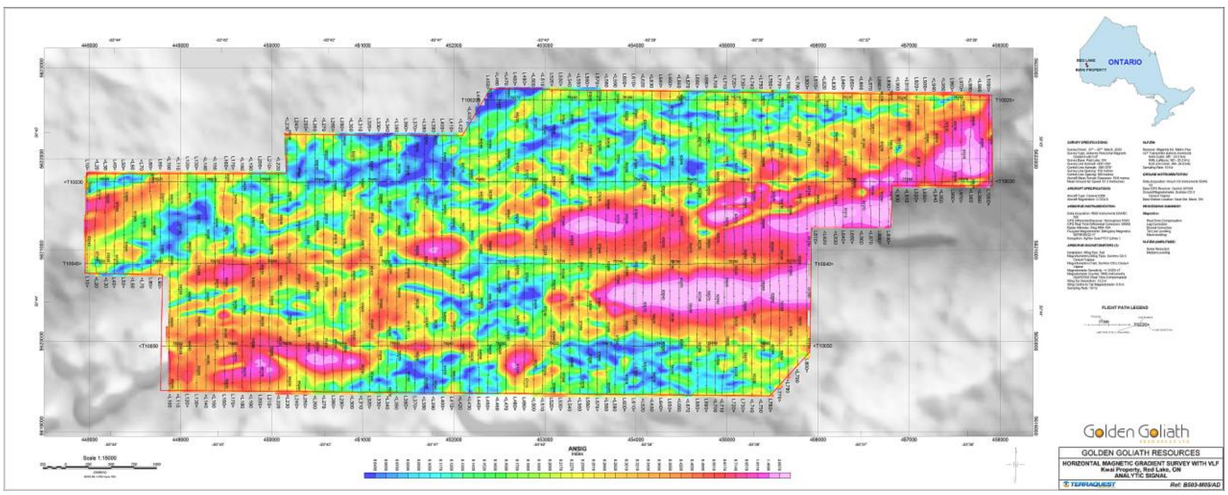

6. Measured Horizontal East-West Magnetic Gradient

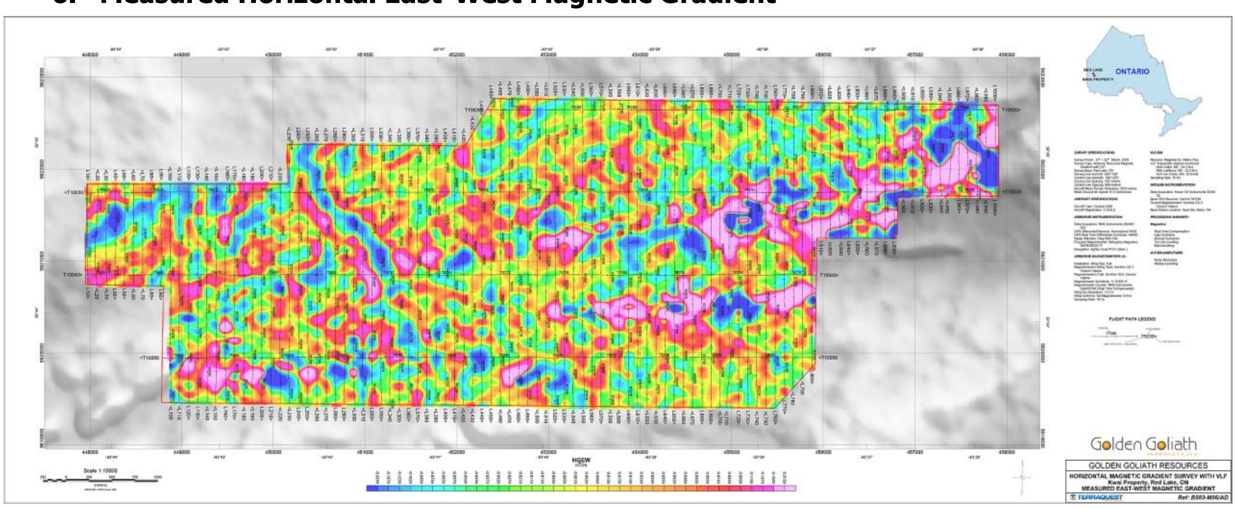

7. Measured Horizontal North-South Magnetic Gradient

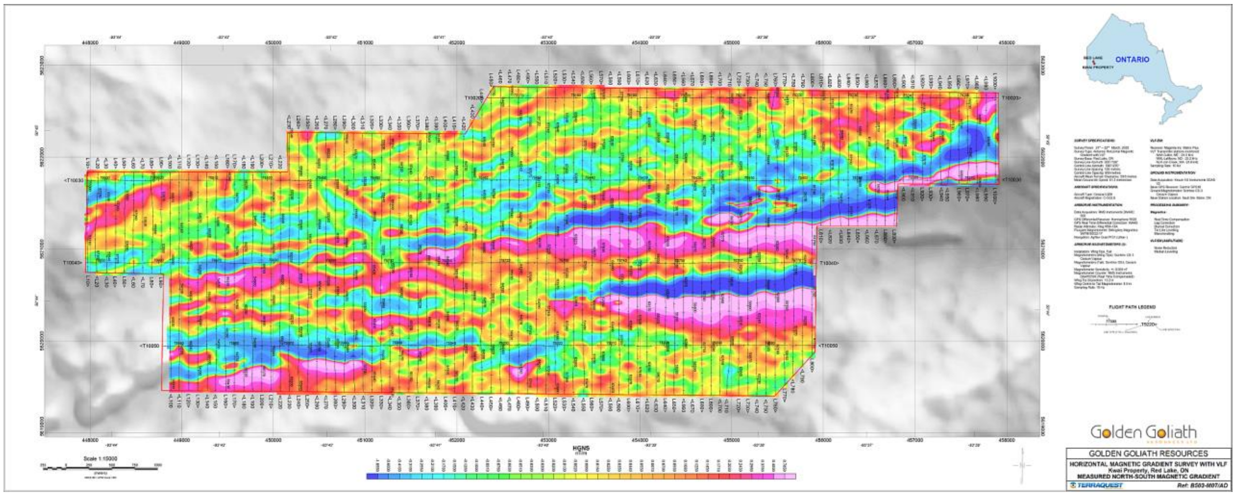

8. Reconstructed Total Magnetic Field

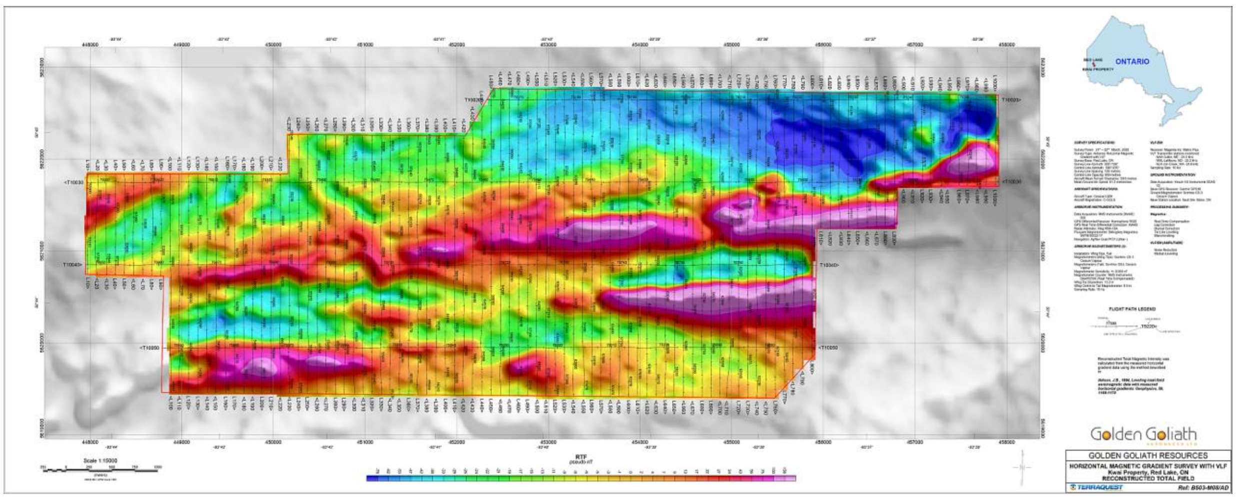

6.5. ELECTROMAGNETC TOTAL FIELD DATA PROCESSING

1. Matrix VLF-EM Monitoring

VLF-EM data were captured using a Magenta Inc. Matrix Digital VLF receiver. This instrument is capable of simultaneously monitoring up to four VLF frequencies, recording amplitude (secondary field), transmitter station azimuth (relative to aircraft orientation), vertical and planar ellipticities and field tilt angle. For this project, the following VLF transmitters were monitored:

- Station NAA: Cutler, Maine – 24.0 kHz
- Station NML: La Moure, North Dakota – 25.2 kHz
- Station NLK: Jim Creek, Washington – 24.8 kHz

Transmitter power, distances and azimuths relative to the survey block are illustrated the Figure on the next page. Transmitter stations are nominally shut down for scheduled maintenance as follows: NAA Cutler, Maine on

Mondays, NML LaMoure, North Dakota on parts of Tuesdays, and NLK Seattle, Washington progressively throughout Wednesday such that there is generally always some signal. Deviations to this schedule are not uncommon.

The survey was flown in a manner that ensures as much as possible that adjacent lines do not have the same VLF Transmitter-off day (see discussion in section 6.2), this ensures that there no significant gaps in the recorded VLF data since the long wavelength of the VLF signal readily crosses three or more survey lines.

2. Matrix VLF-EM Processing Total Field

The *Total Field Amplitude* was processed and presented separately for each of the frequencies. Processing of the raw amplitude data consisted of the following:

- Mask out any embedded "off-line" data
- Noise reduction filtering using non-linear Naudy filtering (5 pt filter width)
- Initial leveling (mean subtraction)
- Fine leveling (micro-leveling)
- Application of bias offsets such that finalized data ranged positive

The finalised amplitude data for each channel were presented as a series of colour images of total field strength (amplitude). Conductor axes and other VLF anomalous features (topographic effects, conductive lake sediments, etc.) are mapped by "hot" colours (light brown -> white) as peak centric lineaments.

Final corrected Amplitude data were high-pass filtered (30 fid cut-off) and used to create data grids which were analysed with a peak-detection algorithm (Blakely algorithm). The resulting peak locations were marked and superimposed on the amplitude images to emphasize conductor axes.

The orientation and distances of the primary fields are located on the legend of each Matrix VLF-EM Total Field conductivity map. The final grids were created using bidirectional (Akima) data interpolations at a cell size of 25 m.

VLF STATION AZIMUTH – B503 Survey

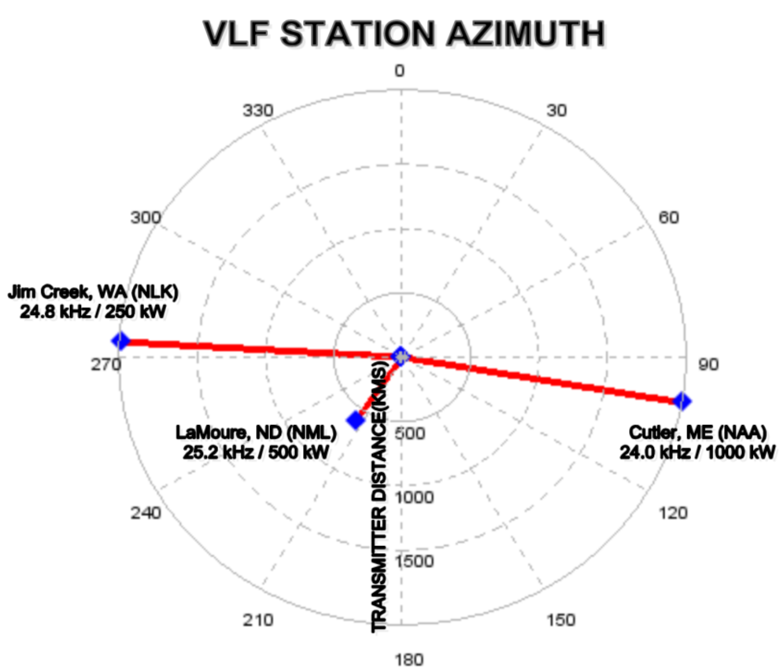

6.6. MATRIX VLF-EM TOTAL FIELD STRENGTH MAPS

1. Amplitude of the Secondary Total Field Strength (NAA, Cutler, ME)

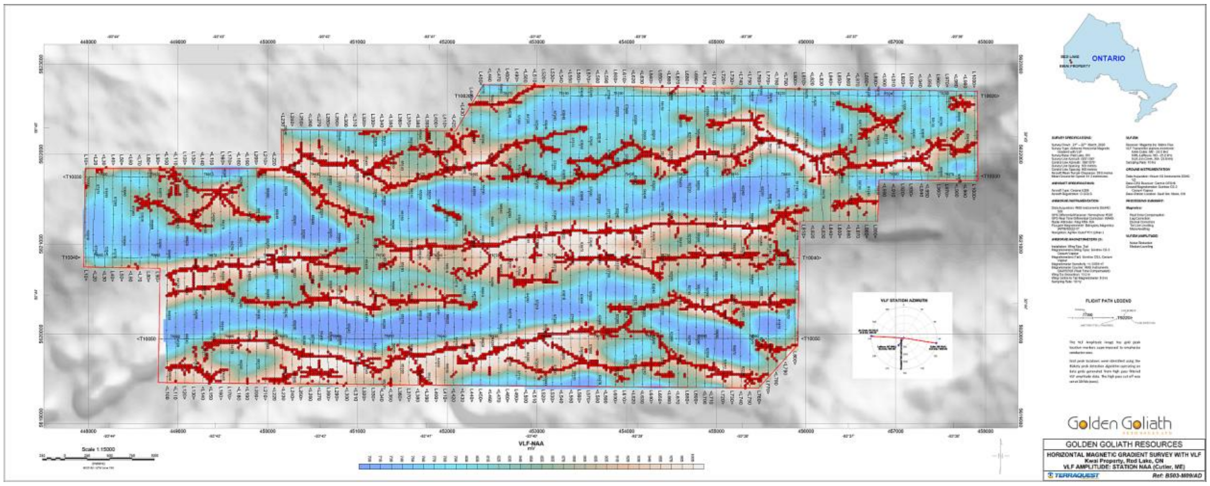

2. Amplitude of the Secondary Total Field Strength (NML, La Moure, ND)

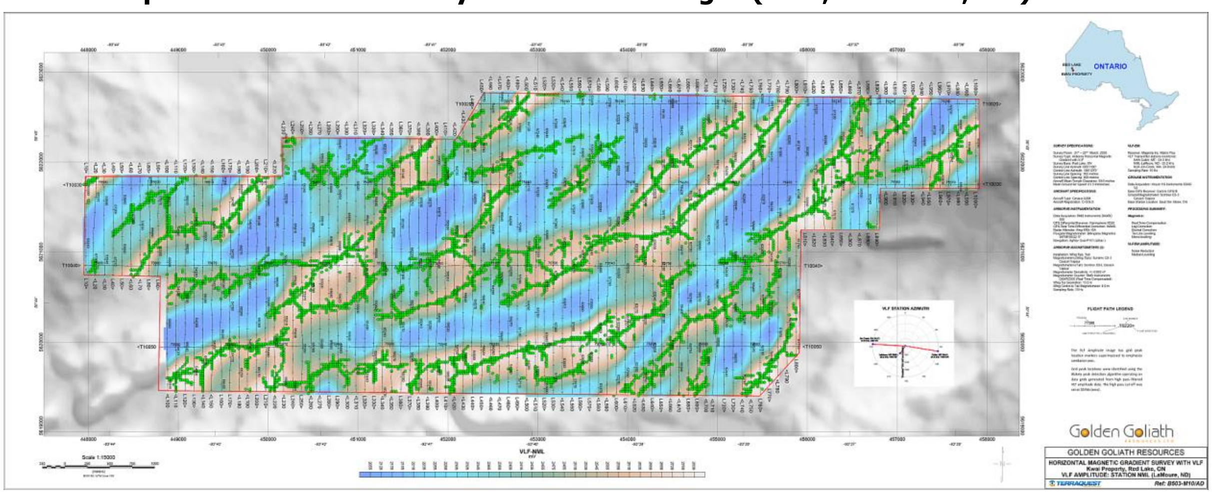

3. Amplitude of the Secondary Total Field Strength (NLK, Jim Creek, WA)

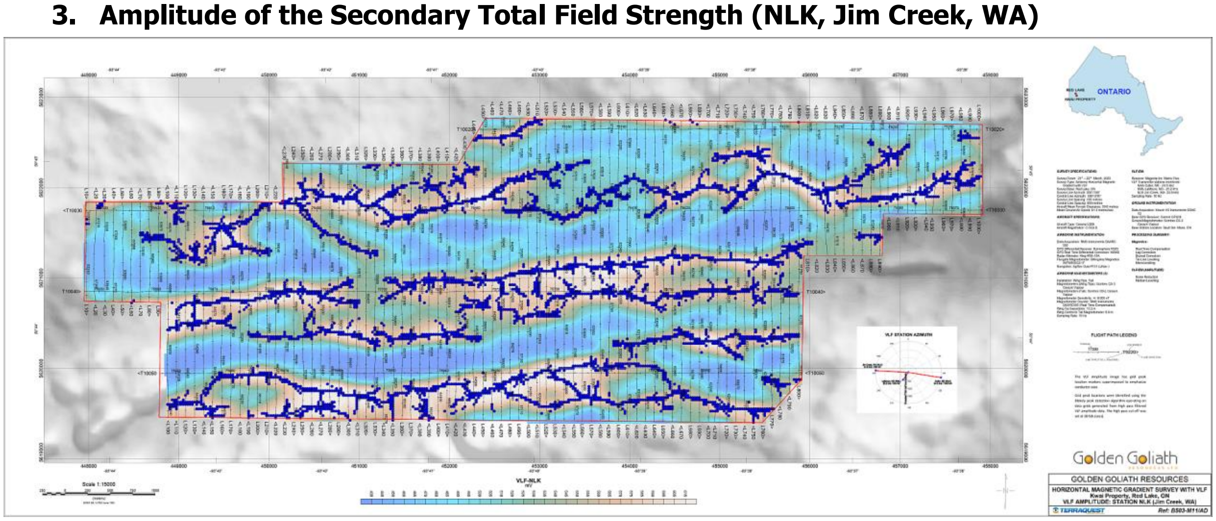

6.7. MATRIX VLF-EM OPTIONAL INVERSE MODELLING

1. Introduction

Based on the quality of the Matrix data on this survey and correlation with airborne magnetic and ground data, the client requested to have the data inverted to calculate the resistivity. The final processed Total Field Strength and all recorded parameters were sent to EMTOMO to perform recently developed inversion procedures designed specifically for airborne VLF-EM data. Products from this processing include a resistivity channel in the database from which resistivity depth slices can be calculated at 0, 5, 10, 20, 40, 60 and 100m depths for Cutler, La Moure and Jim Creek stations. These were final leveled and gridded with 10 metre grid cell size by Terraquest Ltd. and provided as grids for each depth slice. The depth slices have been stacked as three-dimensional montages shown in section 6.8 and presented as final plots for each station. Also, Geosoft VOXELS of resistivity for each VLF transmitter were created and included in the final archive (README file 7.3); these are best visualized on a computer using 3D rotatable software to select desired parameters and views. For purposes of this report examples of 2D rendering of 3D iso-surfaces views are shown in Section 6.9 for Cutler and La Moure transmitters (Cutler and Seattle provide similar but opposite azimuths of energization). A summary of inversion theory follows.

2. Inversion Processing

The VLF signal used in prospection is generated by communication antennas working in the frequency range of 10 kHz to 30 kHz. Those antennas behave like electric dipoles and its associated electromagnetic field (primary field) travels radially outward via two propagation mechanisms: along the earth's surface (wave guided) and by reflection at various charged layers in the ionosphere at altitudes of 60-400 km. The variable primary field induces electrical currents, mainly in conductive structures orientated parallel to the direction the electric field source (VLF transmitter). The induced currents generate an electromagnetic field (secondary field) that can be detected at surface or at some height by the receiver. Having a vertical component of the magnetic field, the following relationship exists between horizontal and vertical components:

$$H_z = T_{zy} H_y$$

where T_{zy} is the magnetic transference function or Tipper. In VLF-EM, the data are the In-phase and Quadrature, or the real and imaginary parts of the tipper (H_z^s/H_y), where H_z^s and H_y are the vertical component of the secondary field and the horizontal component of the total magnetic field.

The nonlinear, smoothness-constrained inversion algorithm (Sasaki, 1989, 2001; DeGroot and Constable, 1990) was adopted for VLF inversion (Monteiro Santos et al., 2006). The inversion is performed by an iterative process that allows the final model to be obtained, with its response fitting the data set in a least square sense. At each iteration, the optimization equations that must be solved to get the corrections of the parameters are represented as follows:

$$(\mathbf{J}^T \mathbf{J} + \lambda \mathbf{C}^T \mathbf{C})\, \delta\vec{p} = \mathbf{J}^T \vec{b}$$

where $\delta\vec{p}$ is the vector containing the corrections applicable to the parameters (logarithm of block conductivity, σ_j) of an initial model, $\vec{b} = \overrightarrow{T^o} - T_i^c$ is the vector of the differences between the observed and calculated tipper components, **J** is the Jacobian matrix whose elements are given by $(\sigma_j)(\partial T_i^c/\partial\sigma_j)$, the superscript T denotes the transpose operation, and λ is a Lagrange multiplier (Damping factor) that controls the amplitude of the parameter corrections and whose best value is determined empirically. The elements of the matrix **C** are the coefficients of the values of the roughness in each parameter, which is defined in terms of the four neighbours' parameters.

DeGroot-Hedlin C. and Constable S.C., 1990. Occam's inversion to generate smooth, two-dimensional models from magnetotelluric data. Geophysics, 55, 1613-1624.

Monteiro Santos, F.A., António Mateus, Jorge Figueiras, Mário A. Gonçalves, 2006. Mapping groundwater contamination around a landfill facility using the VLF-EM method – a case study. Journal of Applied Geophysics.

Sasaki Y., 1989. Two-dimensional joint inversion of magnetotelluric and dipole-dipole resistivity data. Geophysics, 54, 254-262.

6.8. MATRIX VLF-EM RESISTIVITY MAPS

1. Montage of MATRIX VLF-EM Resistivity Depth Slices from Station NAA, Cutler, ME

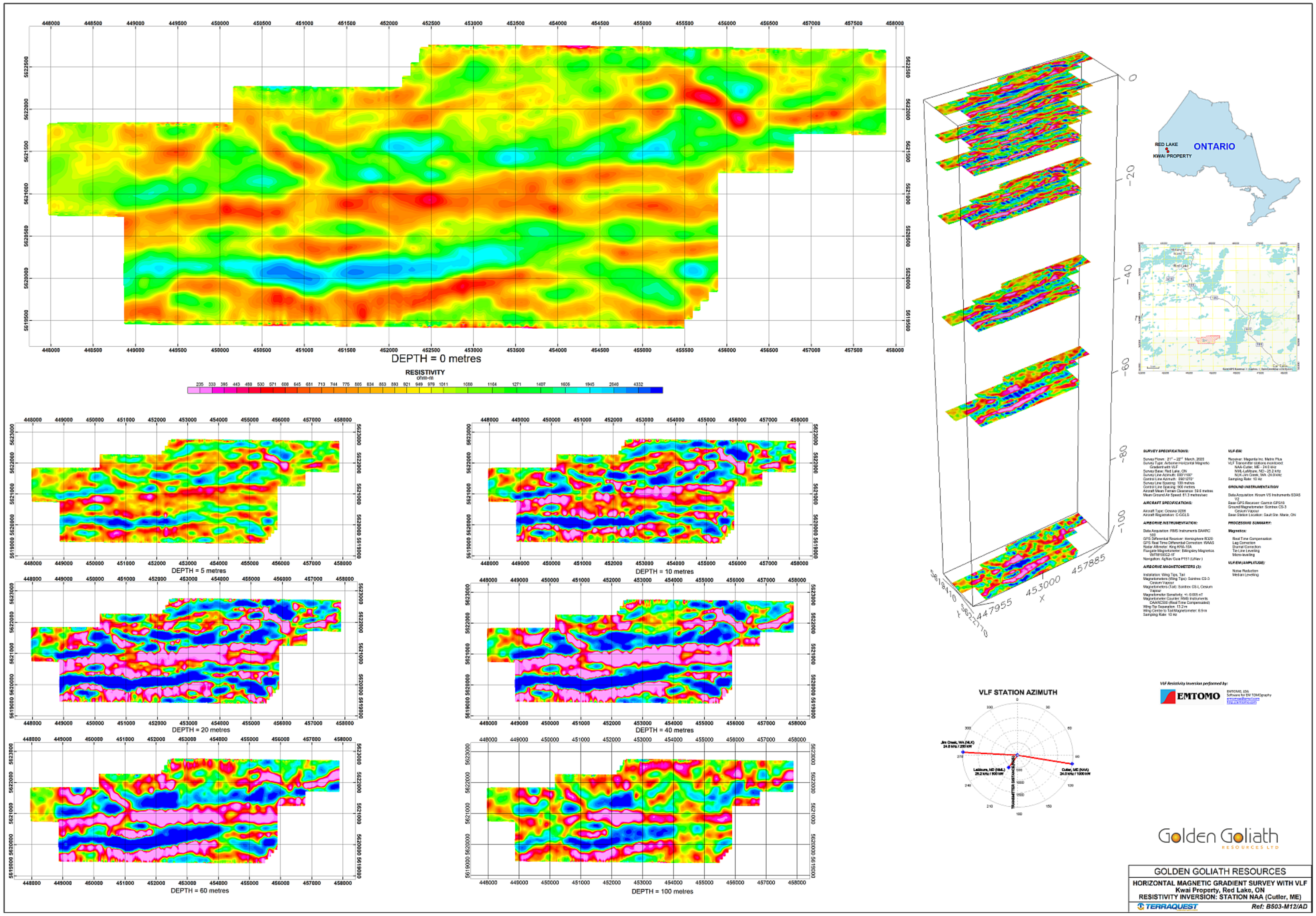

2. Montage of MATRIX VLF-EM Resistivity Depth Slices from Station NML, La Moure, ND

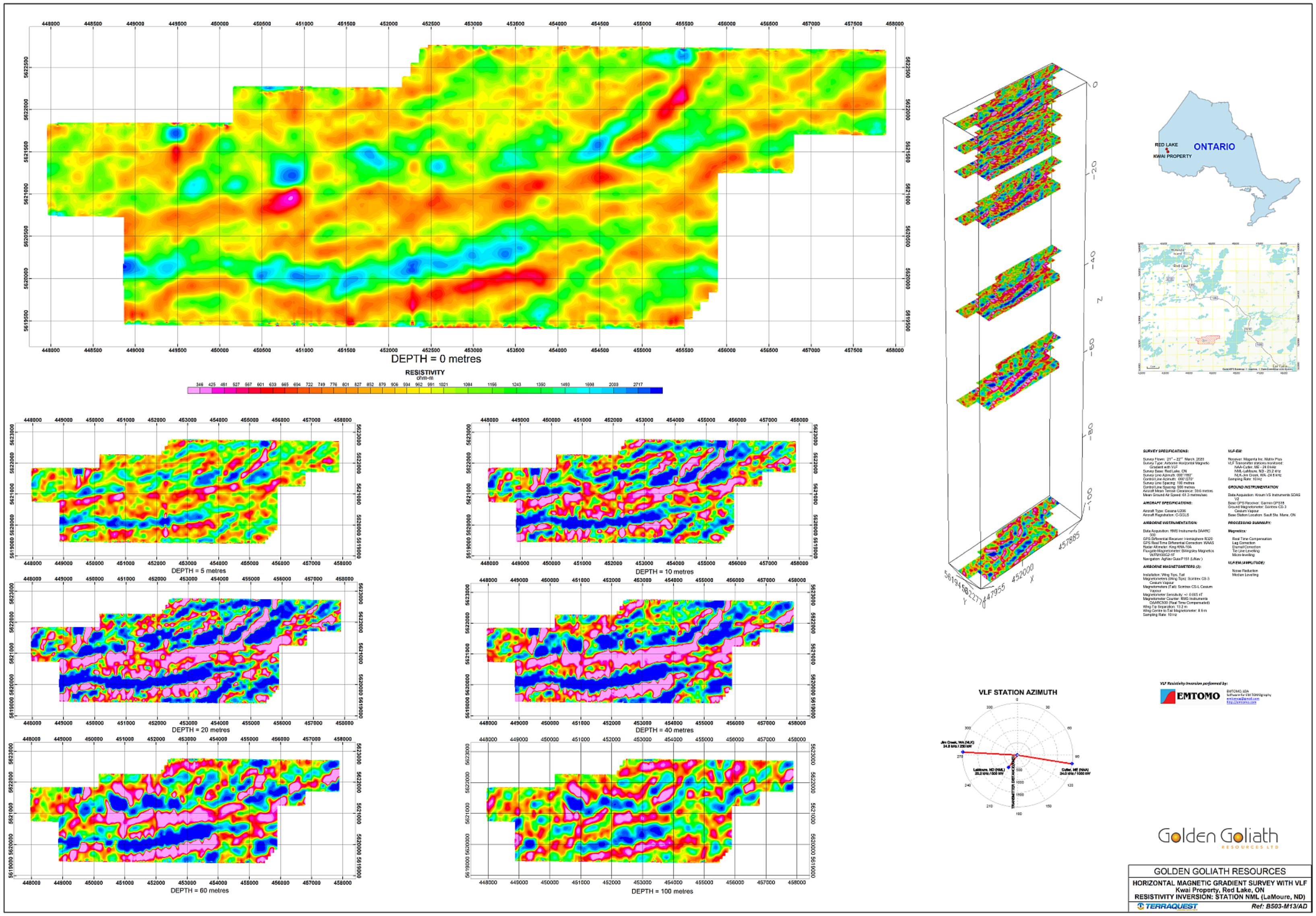

3. Montage of MATRIX VLF-EM Resistivity Depth Slices from Station NLK, Jim Creek, WA

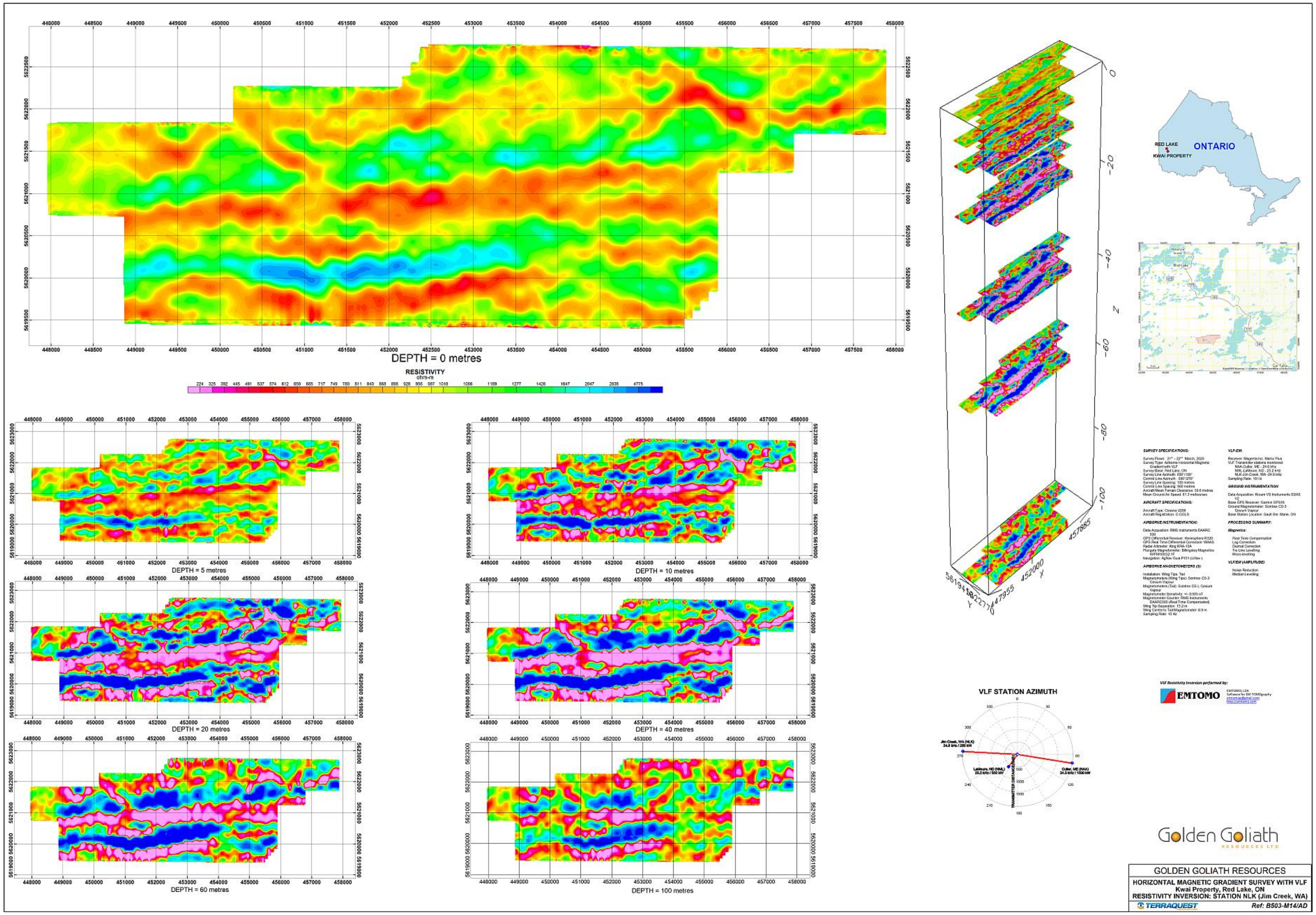

6.9. MATRIX VLF-EM Resistivity - Examples of 3D Iso-Surface Views

1. Cutler NAA Resistivity Voxel: 250 ohm-m level and less

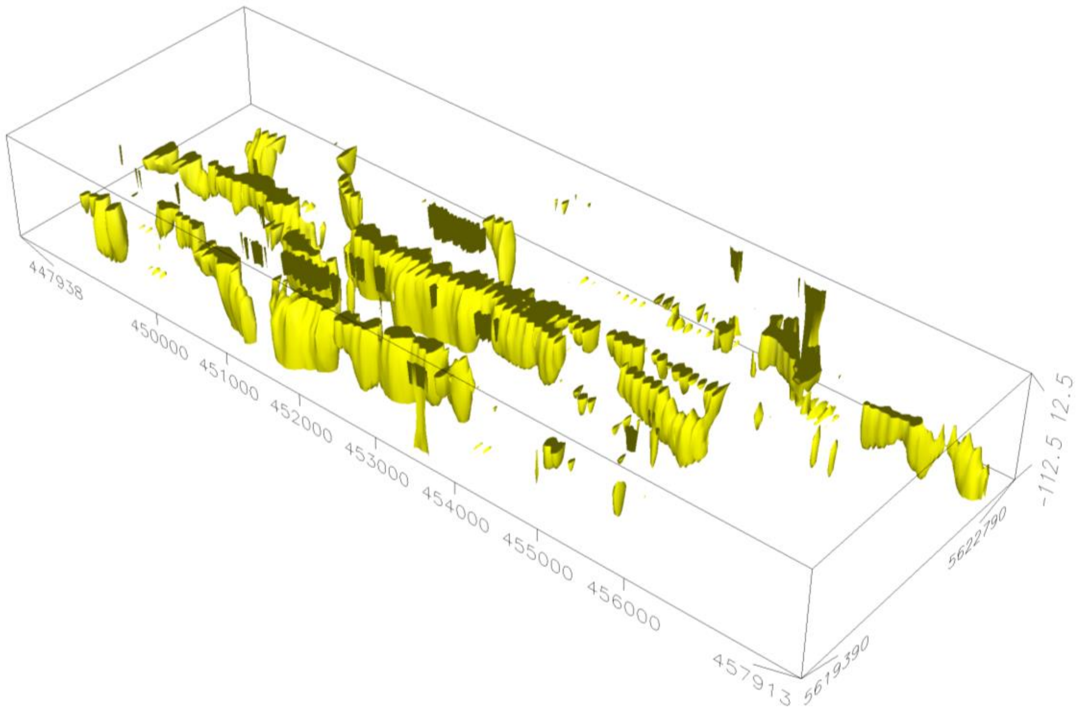

2. Cutler NAA Resistivity Voxel: 250 ohm-m level and less, Zoomed In

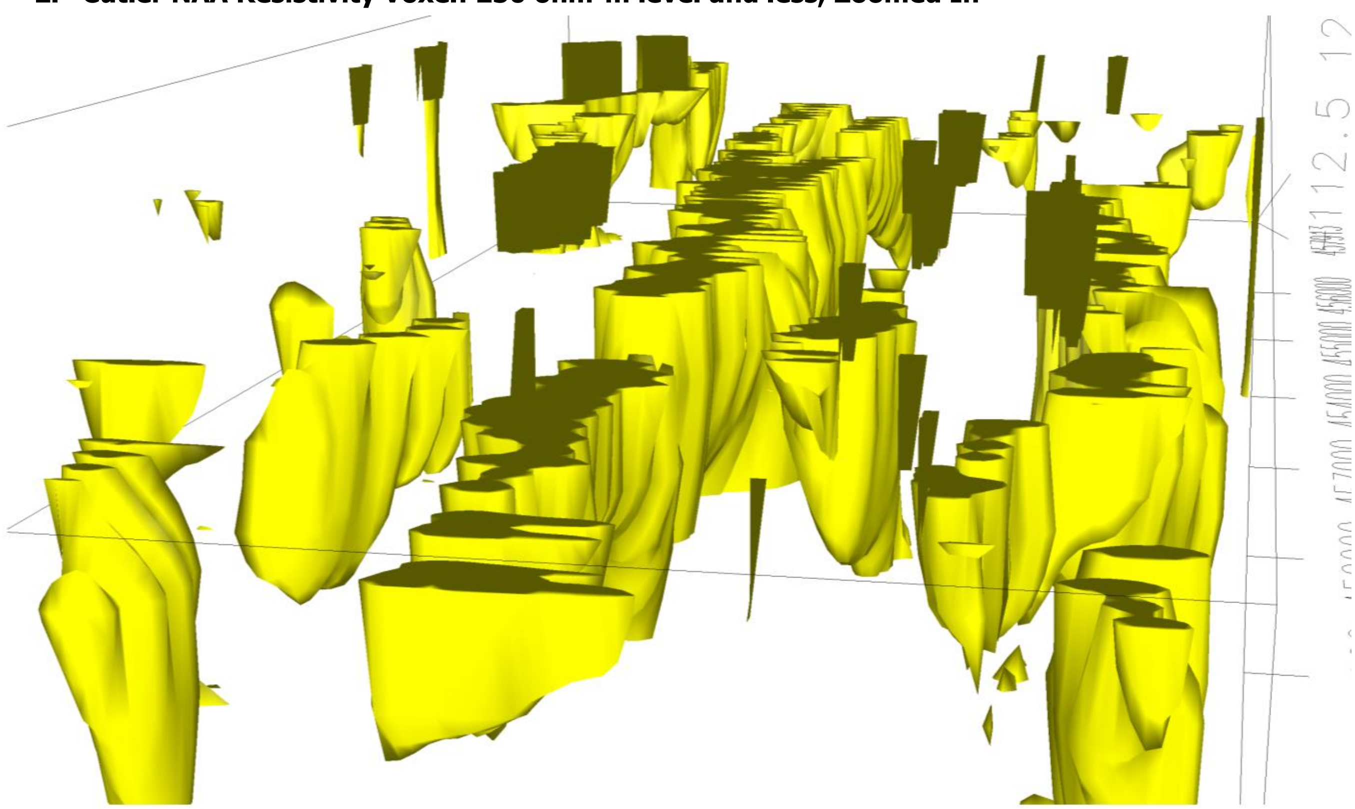

3. La Moure NML Resistivity Voxel: 400 ohm-m level and less

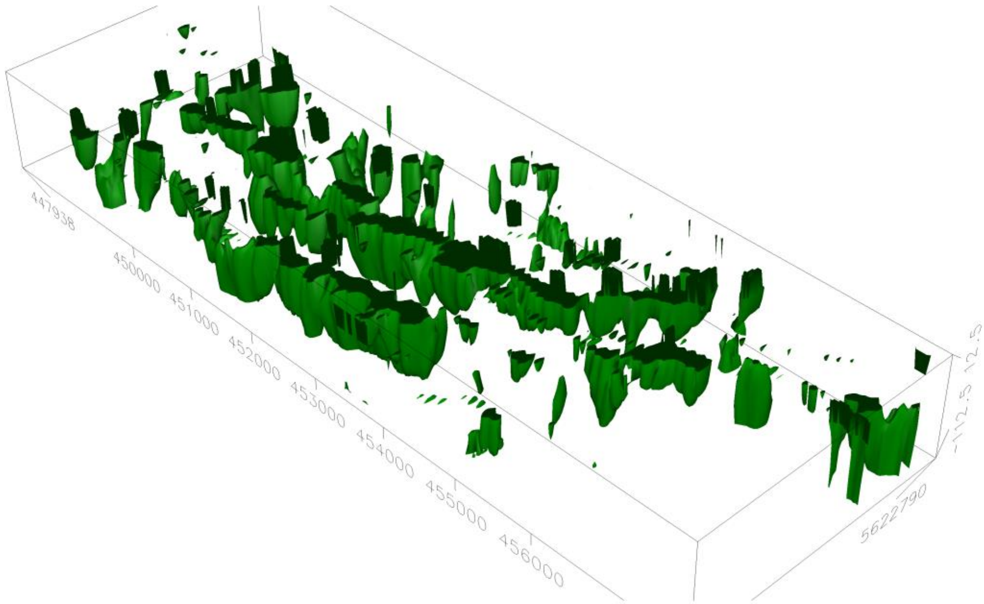

4. La Moure NML Resistivity Voxel: 400 ohm-m level and less, Zoomed In

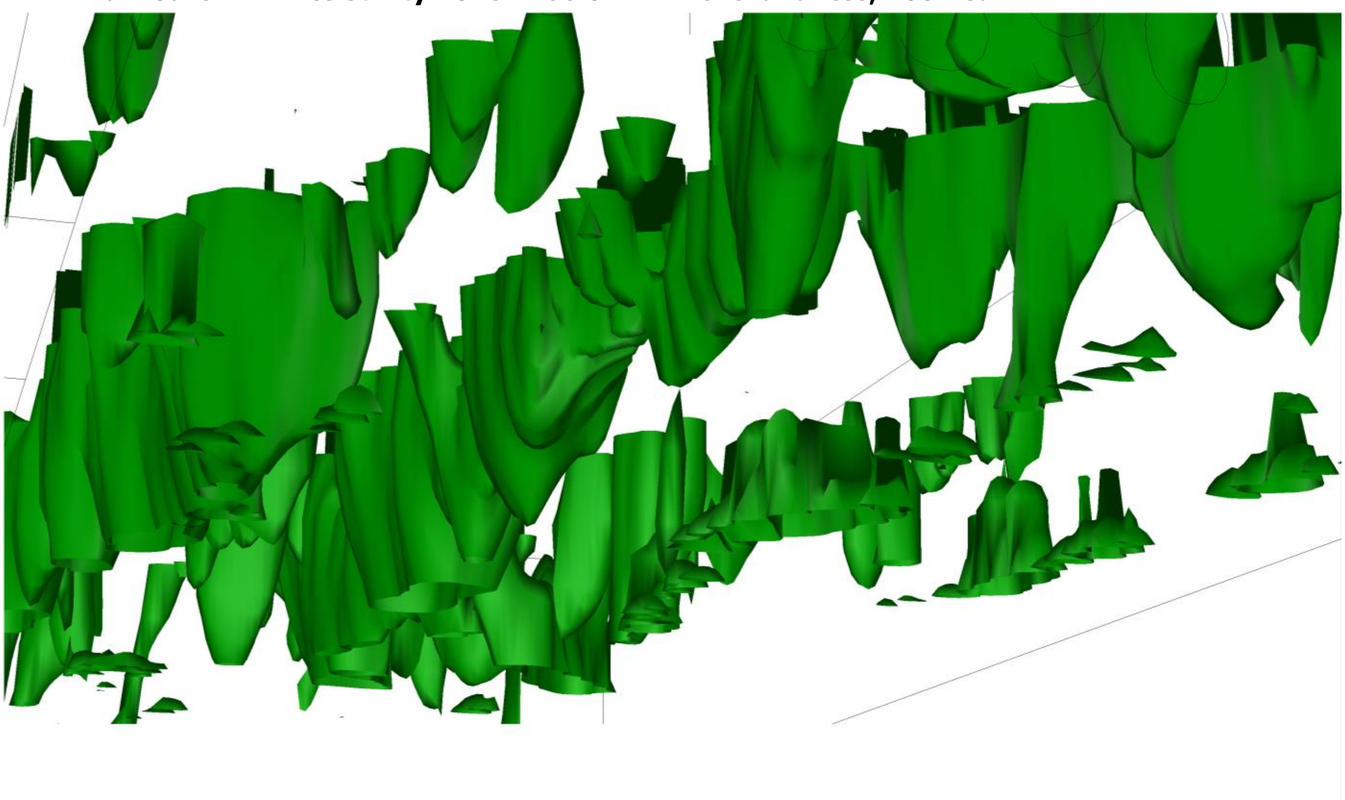

6.10. LIST OF FINAL PRODUCTS

A complete list of all final products is listed in the ReadMe file Appendix 8.3. All products including this Report are contained on an Archive DVD.

The following maps were produced in digital format (PNG) in Low Resolution for the Operations Report, and High Resolution for the Archive and Plotted Maps at 1:15,000 scale (1 copy):

1. Digital Terrain Model
2. Total Magnetic Intensity
3. Anomalous (IGRF corrected) Total Field with contours
4. Calculated Vertical Derivative of Total Magnetic Intensity
5. Calculated Analytic Signal
6. Measured Magnetic Horizontal Gradient - East-West
7. Measured Magnetic horizontal Gradient - North-South
8. Reconstructed Total Magnetic Field
9. Amplitude of the Secondary Total VLF-EM Field (NAA, Cutler, ME)
10. Amplitude of the Secondary Total VLF-EM Field (NML, La Moure, ND)
11. Amplitude of the Secondary Total VLF-EM Field (NLK, Jim Creek, WA)
12. VLF-EM Resistivity Depth Slices from Station NAA Cutler, ME
13. VLF-EM Resistivity Depth Slices from Station NML, La Moure, ND
14. VLF-EM Resistivity Depth Slices from Station NLK, Jim Creek, WA

- Geosoft GRID files
- PNG format of map images
- Database in Geosoft GDB format (compatible with 4.1 or higher)
- One copy of all final maps plotted on glossy film
- Operations Report in PDF format
- Readme.txt

7. SUMMARY

An airborne, high sensitivity, horizontal magnetic gradient and Matrix VLF-EM survey was performed over the Kwai Project located approximately 30 km south of the town of Red Lake, Ontario. The survey was comprised of a single block flown with a mean terrain clearance of 59.6 metres. The traverse line interval was 100 metres and control line interval was 900 metres. The aircraft mean speed was 277.2 km/hr (61.3 m/sec); with a data sample rate of 10 Hz the equivalent ground data points are approximately 6.1 metres along the flight lines. The base of operations was at Red Lake airport (CYRL); a high sensitivity magnetic and a GPS base station was setup at a quiet and secure area at the airport. Throughout the survey this base station recorded the diurnal magnetic activity and was synchronized to the airborne data using GPS time. The data were subjected to final processing to produce a digital archive and one glossy colour copy of the following maps:

a) **Digital Terrain Model** with Flight Path
b) **Magnetics:** Total Magnetic Intensity of tail sensor, Anomalous Magnetic Field, Calculated Vertical Derivative, Analytic Signal, Measured Horizontal Gradients (East-West and North-South), Reconstructed Total Magnetic Field
c) **MATRIX VLF-EM**: Amplitude of the Secondary Total Field from i) NAA, Cutler, ME, ii) NML, La Moure, ND and iii) NLK, Jim Creek, WA, and High-Pass Filter Products from all three frequencies.
d) **MATRIX VLF-EM RESISTIVITY**: Inverse Models Plotted as montages of Resistivity Depth Slices at 0, 5, 10, 20, 40, 60 and 100 metres depths separately for NAA Cutler ME, NML La Moure ND and NLK Jim Creek, WA

This report along with the aeromagnetic gradient and total field VLF-EM and resistivity data have been archived as Geosoft databases (GDB), GRID, and MAP (PNG) formats plus a README. A subfolder of the README contains the database, normal grids and 3D voxels of inverted resistivity data interpretation.

High resolution horizontal gradient magnetic data have provided a detailed data set which can be used to improve the magnetic mapping. The Matrix VLF-EM total field products show good correlation with both magnetic and geologic trends and have been successful in identifying and mapping the structural fabric across the survey area. The Matrix VLF-EM data have been inverted to obtain resistivity data channels, grids and map images of depth slices of the inverted VLF-EM, plus voxels to enable 3D viewing of the VLF-EM Resistivity interpretation.

Respectfully Submitted,

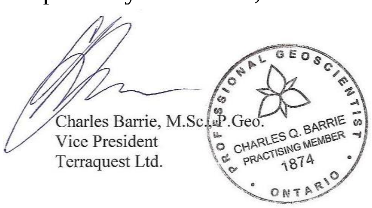

Charles Barrie, M.Sc., P.Geo.
Vice President
Terraquest Ltd.

8. APPENDICES

8.1. APPENDIX I - CERTIFICATE OF QUALIFICATION

I, Charles Q. Barrie, certify that I:

1) am registered as a Fellow with the Geological Association of Canada, as P. Geo. with the Association of Professional Geoscientists of Ontario and work professionally as a geologist,
2) hold an Honours degree in Geology from McMaster University, Canada, obtained in 1977,
3) hold an M.Sc. in Geology from Dalhousie University, Canada, obtained in 1980,
4) am a member of the Prospectors and Developers Association of Canada,
5) am a member of the Canadian Institute of Mining, Metallurgy and Petroleum,
6) have worked as a geologist for forty years,
7) am employed by and am a co-owner of Terraquest Ltd., specializing in high sensitivity airborne geophysical surveys for thirty-four years, and
8) have prepared this operations and specifications report pertaining to airborne data collected by Terraquest Ltd.

Markham, Ontario, Canada

Signed

Charles Barrie, M.Sc., P.Geo.
Vice President
Terraquest Ltd.

8.2.APPENDIX II - MAGNETIC FIGURE OF MERIT (FOM)

GOLDEN GOLIATH / KWAI / SPRING 2020					
Magnetic Figure of Merit Analysis (SRCDAT: 211716 FLIGHT 1979)					
Job Ref:	B503	Date:	21-Mar-20	Aircraft:	C-GGLS
Location :	Red Lake, ON				

Flight Path + Manoevers

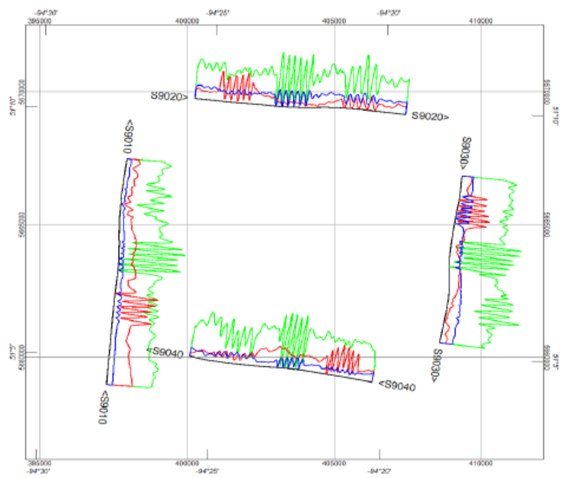

FOM Index : Sensor 1

Calculation note: Residual noise was isolated using a 101 pt Hanning high pass convolution filter with a subsequent low-pass filter (1.0 fid cutoff) applied to reduce non-related HF noise. Individual min-max values determined from the maximum consecutive peak-to-trough residual noise amplitude within each manoevre group

LINE	DIR	TRAV FLG	PITCH MAX	PITCH MIN	ROLL MAX	ROLL MIN	YAW MAX	YAW MIN		P	R	Y	Σ
9010	N	⚑	0.0535	-0.0496	0.0665	-0.0291	0.0509	-0.0575		0.1032	0.0957	0.1084	0.3072
9020	E		0.0717	-0.0221	0.0273	-0.0347	0.0229	-0.0656		0.0938	0.0619	0.0886	0.2443
9030	S	⚑	0.0348	-0.0527	0.0245	-0.0615	-0.0450	-0.1487		0.0874	0.0860	0.1038	0.2772
9040	W		-0.0162	-0.1036	0.0731	-0.0665	0.0884	-0.0799		0.0873	0.1396	0.1683	0.3952
									Σ	0.3717	0.3832	0.4690	1.2239
								Full FOM Index :		1.2239			
								Eq. Traverse FOM Index (Σ Trav x 2) :		1.1688			

FOM Index : Sensor 2

LINE	DIR	TRAV FLG	PITCH MAX	PITCH MIN	ROLL MAX	ROLL MIN	YAW MAX	YAW MIN		P	R	Y	Σ
9010	N	⚑	0.0490	-0.0987	0.0644	-0.0346	0.1040	-0.1138		0.1477	0.0990	0.2179	0.4646
9020	E		0.1300	-0.0867	0.0740	-0.0745	0.1553	-0.2104		0.2167	0.1484	0.3657	0.7308
9030	S	⚑	0.0352	-0.0461	0.0071	-0.0574	-0.0358	-0.1426		0.0814	0.0645	0.1068	0.2526
9040	W		-0.0883	-0.1387	0.0280	-0.0227	0.0259	-0.0645		0.0505	0.0506	0.0904	0.1915
									Σ	0.4961	0.3625	0.7808	1.6395
								Full FOM Index :		1.6395			
								Eq. Traverse FOM Index (Σ Trav x 2) :		1.4343			

FOM Index : Sensor3

LINE	DIR	TRAV FLG	PITCH MAX	PITCH MIN	ROLL MAX	ROLL MIN	YAW MAX	YAW MIN		P	R	Y	Σ
9010	N	⚑	0.0771	0.0016	0.0136	-0.0192	0.0240	-0.0217		0.0755	0.0327	0.0457	0.1539
9020	E		0.0628	-0.0139	0.0020	-0.0254	0.0184	-0.0679		0.0767	0.0274	0.0863	0.1903
9030	S	⚑	0.0253	-0.0595	-0.0037	-0.0143	-0.0909	-0.1207		0.0848	0.0105	0.0298	0.1252
9040	W		-0.0247	-0.0678	0.0183	-0.0217	0.0241	-0.0242		0.0431	0.0401	0.0483	0.1315
									Σ	0.2801	0.1108	0.2100	0.6009
								Full FOM Index :		0.6009			
								Eq. Traverse FOM Index (Σ Trav x 2) :		0.5582			

8.3. APPENDIX III – README

```
TERRAQUEST Final Data Archive Documentation
===========================================

TERRAQUEST reference : B503

Client: Golden Goliath Resources
Project: Kwai Property
Type: Aeromagnetic Gradient Survey /w VLF (Fixed Wing)
Operations: Winter, 2020
Survey Base: Red Lake, ON
Aircraft: Cessna 206
Archive Version: 200814
Prepared By: Allen Duffy

1. Data Organisation:

+---B503ARC_GOLDEN-GOLIATH_200814
|   +---DATA
|   |       B503ARC_GOLDEN-GOLIATH_200814.gdb
|   |
|   +---GRIDS
|   |       ANSIG.grd
|   |       ANSIG.grd.gi
|   |       DTMFNL.grd
|   |       DTMFNL.grd.gi
|   |       HGEW.grd
|   |       HGEW.grd.gi
|   |       HGNS.grd
|   |       HGNS.grd.gi
|   |       NAA_AMP.grd
|   |       NAA_AMP.grd.gi
|   |       NAA_AMP_HP.grd
|   |       NAA_AMP_HP.grd.gi
|   |       NAA_PEAK_OVERLAY.grd
|   |       NAA_PEAK_OVERLAY.grd.gi
|   |       NLK_AMP.grd
|   |       NLK_AMP.grd.gi
|   |       NLK_AMP_HP.grd
|   |       NLK_AMP_HP.grd.gi
|   |       NLK_PEAK_OVERLAY.grd
|   |       NLK_PEAK_OVERLAY.grd.gi
|   |       NML_AMP.grd
|   |       NML_AMP.grd.gi
|   |       NML_AMP_HP.grd
|   |       NML_AMP_HP.grd.gi
|   |       NML_PEAK_OVERLAY.grd
|   |       NML_PEAK_OVERLAY.grd.gi
|   |       RTF.grd
|   |       RTF.grd.gi
|   |       TF3ANM.grd
|   |       TF3ANM.grd.gi
|   |       TF3FNL.grd
|   |       TF3FNL.grd.gi
|   |       TF3VD1.grd
|   |       TF3VD1.grd.gi
|   |
|   +---MAPS
|   |   |   B503_GOLDENGOLIATH_KWAI_M01_FPwDTM.png
|   |   |   B503_GOLDENGOLIATH_KWAI_M02_TMI.png
|   |   |   B503_GOLDENGOLIATH_KWAI_M03_TMIANM.png
|   |   |   B503_GOLDENGOLIATH_KWAI_M04_TMIVD1.png
|   |   |   B503_GOLDENGOLIATH_KWAI_M05_ANSIG.png
|   |   |   B503_GOLDENGOLIATH_KWAI_M06_HGEW.png
|   |   |   B503_GOLDENGOLIATH_KWAI_M07_HGNS.png
|   |   |   B503_GOLDENGOLIATH_KWAI_M08_RTF.png
|   |   |   B503_GOLDENGOLIATH_KWAI_M09_VLFNAA.png
|   |   |   B503_GOLDENGOLIATH_KWAI_M10_VLFNML.png
|   |   |   B503_GOLDENGOLIATH_KWAI_M11_VLFNLK.png
|   |   |   B503_GOLDENGOLIATH_KWAI_M12_RESIST_NAA.png
|   |   |   B503_GOLDENGOLIATH_KWAI_M13_RESIST_NML.png
|   |   |   B503_GOLDENGOLIATH_KWAI_M14_RESIST_NLK.png
|   |   |
```

```
|   |   \---LORES
|   |           B503_GOLDENGOLIATH_KWAI_M01_FPwDTM.png
|   |           B503_GOLDENGOLIATH_KWAI_M02_TMI.png
|   |           B503_GOLDENGOLIATH_KWAI_M03_TMIANM.png
|   |           B503_GOLDENGOLIATH_KWAI_M04_TMIVD1.png
|   |           B503_GOLDENGOLIATH_KWAI_M05_ANSIG.png
|   |           B503_GOLDENGOLIATH_KWAI_M06_HGEW.png
|   |           B503_GOLDENGOLIATH_KWAI_M07_HGNS.png
|   |           B503_GOLDENGOLIATH_KWAI_M08_RTF.png
|   |           B503_GOLDENGOLIATH_KWAI_M09_VLFNAA.png
|   |           B503_GOLDENGOLIATH_KWAI_M10_VLFNML.png
|   |           B503_GOLDENGOLIATH_KWAI_M11_VLFNLK.png
|   |           B503_GOLDENGOLIATH_KWAI_M12_RESIST_NAA.png
|   |           B503_GOLDENGOLIATH_KWAI_M13_RESIST_NML.png
|   |           B503_GOLDENGOLIATH_KWAI_M14_RESIST_NLK.png
|   |
|   +---README
|   |       B503ARC_GOLDEN-GOLIATH.ReadMe
|   |
|   +---REPORT
|   \---VLF_INTERP
|       +---NAA
|       |   +---GRIDS
|       |   |       NAA_RES_000_FNL.grd
|       |   |       NAA_RES_000_FNL.grd.gi
|       |   |       NAA_RES_005_FNL.grd
|       |   |       NAA_RES_005_FNL.grd.gi
|       |   |       NAA_RES_010_FNL.grd
|       |   |       NAA_RES_010_FNL.grd.gi
|       |   |       NAA_RES_020_FNL.grd
|       |   |       NAA_RES_020_FNL.grd.gi
|       |   |       NAA_RES_040_FNL.grd
|       |   |       NAA_RES_040_FNL.grd.gi
|       |   |       NAA_RES_060_FNL.grd
|       |   |       NAA_RES_060_FNL.grd.gi
|       |   |       NAA_RES_100_FNL.grd
|       |   |       NAA_RES_100_FNL.grd.gi
|       |   |
|       |   +---GRID_GDB
|       |   |       NAA_RES_GRIDS.gdb
|       |   |
|       |   +---PROFILE_GDB
|       |   |       NAA_RES_PROFILE.gdb
|       |   |
|       |   \---VOXEL
|       |           NAA_RES_GRIDS_RES.geosoft_voxel
|       |
|       +---NLK
|       |   +---GRIDS
|       |   |       NLK_RES_000_FNL.grd
|       |   |       NLK_RES_000_FNL.grd.gi
|       |   |       NLK_RES_005_FNL.grd
|       |   |       NLK_RES_005_FNL.grd.gi
|       |   |       NLK_RES_010_FNL.grd
|       |   |       NLK_RES_010_FNL.grd.gi
|       |   |       NLK_RES_020_FNL.grd
|       |   |       NLK_RES_020_FNL.grd.gi
|       |   |       NLK_RES_040_FNL.grd
|       |   |       NLK_RES_040_FNL.grd.gi
|       |   |       NLK_RES_060_FNL.grd
|       |   |       NLK_RES_060_FNL.grd.gi
|       |   |       NLK_RES_100_FNL.grd
|       |   |       NLK_RES_100_FNL.grd.gi
|       |   |
|       |   +---GRID_GDB
|       |   |       NLK_RES_GRIDS.gdb
|       |   |
|       |   +---PROFILE_GDB
|       |   |       NLK_RES_PROFILE.gdb
|       |   |
|       |   \---VOXEL
|       |           NLK_RES_GRIDS_RES.geosoft_voxel
|       |
|       +---NML
|       |   +---GRIDS
|       |   |       NML_RES_000_FNL.grd
|       |   |       NML_RES_000_FNL.grd.gi
|       |   |       NML_RES_005_FNL.grd
|       |   |       NML_RES_005_FNL.grd.gi
```

```
|       |   |       NML_RES_010_FNL.grd
|       |   |       NML_RES_010_FNL.grd.gi
|       |   |       NML_RES_020_FNL.grd
|       |   |       NML_RES_020_FNL.grd.gi
|       |   |       NML_RES_040_FNL.grd
|       |   |       NML_RES_040_FNL.grd.gi
|       |   |       NML_RES_060_FNL.grd
|       |   |       NML_RES_060_FNL.grd.gi
|       |   |       NML_RES_100_FNL.grd
|       |   |       NML_RES_100_FNL.grd.gi
|       |   |
|       |   +---GRID_GDB
|       |   |       NML_RES_GRIDS.gdb
|       |   |
|       |   +---PROFILE_GDB
|       |   |       NML_RES_PROFILE.gdb
|       |   |
|       |   \---VOXEL
|       |           NML_RES_GRIDS_RES.geosoft_voxel
|       |
|       \---README
|               B503ARC_VLF_INTERP.ReadMe

2.  Database Contents: "B503ARC_GOLDEN-GOLIATH_200814.gdb"

    Data sampled at 10Hz ...

    X_UTM_WIN       : UTM Easting - WGS84, UTM Zone 15N (metres)
    Y_UTM_WIN       : UTM Easting - WGS84, UTM Zone 15N (metres)
    Flight          : Flight Number
    DATE            : Flight Date (DD/MM/YYYY format - ASCII)
    AZIMUTH         : Flight line direction (ranged 0 - 360 degrees)
    FID             : Fiducial (UTC seconds)
    TIME            : UTC TIME (hh:mm:ss.ss format)
    RADAR           : Radar Altimeter (metres AGL)
    ALT             : WGS84 Altitude (metres AMSL)
    LAT             : Latitude (degrees)
    LON             : Longitude (degrees)
    DTMFNL          : Calculated Digital Terrain model (m AMSL)
    DIURNAL         : Raw Diurnal (nT)
    DIUEDIT         : Edited Diurnal (culture removed, nT)
    VMX             : Fluxgate X component (nT)
    VMY             : Fluxgate Y component (nT)
    VMZ             : Fluxgate Z component (nT)
    TF1UNC          : Raw measured TMI (nT) - Left Wing
    TF2UNC          : Raw measured TMI (nT) - Right Wing
    TF3UNC          : Raw measured TMI (nT) - Tail
    TF1CMP          : Compensated TMI (nT) - Left Wing
    TF2CMP          : Compensated TMI (nT) - Right Wing
    TF3CMP          : Compensated TMI (nT) - Tail
    TF1CMPEDIT      : Edited (spikes removed), Compensated TMI (nT) - Left Wing
    TF2CMPEDIT      : Edited (spikes removed), Compensated TMI (nT) - Right Wing
    TF3CMPEDIT      : Edited (spikes removed), Compensated TMI (nT) - Tail
    HGEWML_LAG      : Measured East-West Magnetic gradient (nT/m), lag corrected
    HGNSML_LAG      : Measured North-South Magnetic gradient (nT/m), lag corrected
    TF3LAG          : Lag corrected TF3 (Tail TMI)
    TF3DIU          : Diurnal Corrected Total Magnetic Field (Tail TMI, nT)
    TF3LVL          : Tie-line levelled Total Magnetic Field (Tail TMI, nT)
    TF3FNL          : Final, micro-levelled Total Magnetic Field (Tail TMI, nT)
    SER06_AMP1      : Raw VLF Amplitude (Station NAA, Cutler, Maine)
    SER06_DIR1      : Raw VLF Azimuth (Station NAA, Cutler, Maine)
    SER06_EP1       : Raw VLF Planar Ellipticity (Station NAA, Cutler, Maine)
    SER06_EV1       : Raw VLF Vertical Ellipticity (Station NAA, Cutler, Maine)
    SER06_TLT1      : Raw VLF Tilt Angle (Station NAA, Cutler, Maine)
    SER06_AMP2      : Raw VLF Amplitude (Station NML, LaMoure, North Dakota)
    SER06_DIR2      : Raw VLF Azimuth (Station NML, LaMoure, North Dakota)
    SER06_EP2       : Raw VLF Planar Ellipticity (Station NML, LaMoure, North Dakota)
    SER06_EV2       : Raw VLF Vertical Ellipticity (Station NML, LaMoure, North Dakota)
    SER06_TLT2      : Raw VLF Tilt Angle (Station NML, LaMoure, North Dakota)
    SER06_AMP3      : Raw VLF Amplitude (Station NLK, Jim Creek, Washington)
    SER06_DIR3      : Raw VLF Azimuth (Station NLK, Jim Creek, Washington)
    SER06_EP3       : Raw VLF Planar Ellipticity (Station NLK, Jim Creek, Washington)
    SER06_EV3       : Raw VLF Vertical Ellipticity (Station NLK, Jim Creek, Washington)
    SER06_TLT3      : Raw VLF Tilt Angle (Station NLK, Jim Creek, Washington)
    NAA_LAG         : Processed VLF Amplitude (Total Field) - Station NAA (Cutler, Maine)
    NAA_LAG_HP      : Processed VLF Amplitude (HP filtered) - Station NAA (Cutler, Maine)
    NML_LAG         : Processed VLF Amplitude (Total Field) - Station NML (LaMoure, North Dakota)
    NML_LAG_HP      : Processed VLF Amplitude (HP filtered) - Station NML (LaMoure, North Dakota)
    NLK_LAG         : Processed VLF Amplitude (Total Field) - Station NLK (Jim Creek, Washington)
```

```
   NLK_LAG_HP      : Processed VLF Amplitude (HP filtered) - Station NLK (Jim Creek, Washington)
   IP1_LAG_ML      : Final In-Phase (from Tilt Angle)) - Station NAA (Cutler, Maine)
   QD1_LAG_ML      : Final Quadrature (from Vertical Ellipticity)) - Station NAA (Cutler, Maine)
   IP2_LAG_ML      : Final In-Phase (from Tilt Angle)) - Station NML (Lamoure, North Dakota)
   QD2_LAG_ML      : Final Quadrature (from Vertical Ellipticity)) - Station NML (Lamoure, North Dakota)
   IP3_LAG_ML      : Final In-Phase (from Tilt Angle)) - Station NLK (Jim Creek, Washington)
   QD3_LAG_ML      : Final Quadrature (from Vertical Ellipticity)) - Station NLK (Jim Creek, Washington)

3.  GRIDS

   Grids prepared using Bi-Directional (Akima) spline with a 25m grid cell size

   DTMFNL.grd             :  Digital Terrain Model (m AMSL)
   HGEW.grd               :  Measured East-West Horizontal Magnetic Gradient (nT/m)
   HGNS.grd               :  Measured North-South Horizontal Magnetic Gradient (nT/m)
   NAA_AMP.grd            :  VLF Amplitude (Total Field) - Station NAA (Cutler, Maine)
   NAA_AMP_HP.grd         :  VLF Amplitude (HP filtered) - Station NAA (Cutler, Maine)
   NLK_AMP.grd            :  VLF Amplitude (Total Field) - Station NML (LaMoure, North Dakota)
   NLK_AMP_HP.grd         :  VLF Amplitude (HP filtered) - Station NML (LaMoure, North Dakota)
   NML_AMP.grd            :  VLF Amplitude (Total Field) - Station NLK (Jim Creek, Washington)
   NML_AMP_HP.grd         :  VLF Amplitude (HP filtered) - Station NLK (Jim Creek, Washington)
   RTF.grd                :  Reconstructed Total Magnetic Field (calculated from Horizontal Gradients, pseudo nT)
   TF3FNL.grd             :  Final, corrected Total Magnetic Field (nT)
   TF3ANM.grd             :  Anomalous (IGRF corrected) Total Magnetic Field (nT)
   TF3VD1.grd             :  Calculated first vertical magnetic derivative (nT/m)
   ANSIG.grd              :  Calculated Analytic Signal
   NAA_PEAK_OVERLAY.grd   :  Conductor Peak Marker Overlay Grid, NAA (Cutler, Maine) (Geosoft Colour grid)
   NML_PEAK_OVERLAY.grd   :  Conductor Peak Marker Overlay Grid, NML (LaMoure, North Dakota) (Geosoft Colour grid)
   NLK_PEAK_OVERLAY.grd   :  Conductor Peak Marker Overlay Grid, NLK (Jim Creek, Washington) (Geosoft Colour grid)

4. MAPS

   PNG images of the printed map series in full resolution (300 DPI) and low resolution
   (email-able, files in sub folder 'LORES'). Data are presented on a series of 14 1:15000 scale
   maps:

   B503_GOLDENGOLIATH_KWAI_M01_FPwDTM    : Flight Path with DTM grid
   B503_GOLDENGOLIATH_KWAI_M02_TMI       : Total Magnetic Intensity
   B503_GOLDENGOLIATH_KWAI_M03_TMIANM    : Anomalous (IGRF corrected) Total Field with contours
   B503_GOLDENGOLIATH_KWAI_M04_TMIVD1    : Calculated Vertical Magnetic Derivative
   B503_GOLDENGOLIATH_KWAI_M05_ANSIG     : Calculated Analytic Signal
   B503_GOLDENGOLIATH_KWAI_M06_HGEW      : Measured East-West Magnetic Gradient
   B503_GOLDENGOLIATH_KWAI_M07_HGNS      : Measured North-South Magnetic Gradient
   B503_GOLDENGOLIATH_KWAI_M08_RTF       : Reconstructed Total Field (from Horizontal Gradients)
   B503_GOLDENGOLIATH_KWAI_M09_VLFNAA    : VLF Amplitude (Total Field) - Station NAA (Cutler, Maine)
   B503_GOLDENGOLIATH_KWAI_M10_VLFNML    : VLF Amplitude (Total Field) - Station NML (LaMoure, North Dakota)
   B503_GOLDENGOLIATH_KWAI_M11_VLFNLK    : VLF Amplitude (Total Field) - Station NLK (Jim Creek, Washington)
   B503_GOLDENGOLIATH_KWAI_M12_RESIST_NAA: VLF Resistivity Inversion - Station NAA (Cutler, Maine)
   B503_GOLDENGOLIATH_KWAI_M13_RESIST_NML: VLF Resistivity Inversion - Station NML (LaMoure, North Dakota)
   B503_GOLDENGOLIATH_KWAI_M14_RESIST_NLK: VLF Resistivity Inversion - Station NLK (Jim Creek, Washington)

5. README

   Archive documentation : B503ARC_GOLDEN-GOLIATH.ReadMe (this file)

6. REPORT

   Project Operations report

7. VLF_INTERP

   7.1  Database Contents: PROFILE_GDB

      "xxx_RES_PROFILE.gdb"

      In each main VLF Transmitter folder (NAA, NLK and NML), survey line based data archives are stored in
      sub-folder "PROFILE_GDB". The profile based databases are named "xxx_RES_PROFILE", where "xxx" is NAA, NLK or NML,
      and contain the following data fields:

      Data sampled at 10Hz ...

      X_UTM_WIN       : UTM Easting - WGS84, UTM Zone 15N (metres)
      Y_UTM_WIN       : UTM Easting - WGS84, UTM Zone 15N (metres)
      DATE            : Flight Date (DD/MM/YYYY format - ASCII)
      Flight          : Flight Number
      AZIMUTH         : AZIMUTH (flight line direction, ranged 0-360 deg)
      LNUM            : Line number (numerical value only)
      LTYP            : Line Type (L: Traverse; T: Tie)
      RADLAG          : Radar Altimeter (lag corrected, metres AGL)
```

```
ALT             : WGS84 Altitude (metres AMSL)
DTMFNL          : Digital Terrain Model (metres AMSL)
LAT             : Latitude (degrees)
LON             : Longitude (degrees)
xxx_RES_000     : Resistivity (model inversion) - at surface (ohm-m)
xxx_RES_005     : Resistivity (model inversion) - depth=5 metres (ohm-m)
xxx_RES_010     : Resistivity (model inversion) - depth=10 metres (ohm-m)
xxx_RES_025     : Resistivity (model inversion) - depth=20 metres (ohm-m)
xxx_RES_040     : Resistivity (model inversion) - depth=40 metres (ohm-m)
xxx_RES_060     : Resistivity (model inversion) - depth=60 metres (ohm-m)
xxx_RES_100     : Resistivity (model inversion) - depth=100 metres (ohm-m)
```

7.2 Database Contents: GRID_GDB

"xxx_RES_GRIDS.gdb"

VLF inversion data are also stored in "GRID" format as a series of numerical lattices corresponding to each individual inversion depth (surface, 5, 10, 20, 40, 60 and 100 metres depths). This database format is useful for creating 3D data grids. In each main VLF Transmitter folder (NAA, NLK and NML), "grid" based data archives are stored in sub-folder "GRID_GDB". The grid-based databases are named "xxx_RES_GRIDS", where "xxx" is NAA, NLK or NML. Data are organised into 7 "lines", corresponding to each individual depth plane :

```
DDEPTH000    : Inversion plane at DEPTH=surface XYZ points
DDEPTH005    : Inversion plane at DEPTH=5m XYZ points
DDEPTH010    : Inversion plane at DEPTH=10m XYZ points
DDEPTH025    : Inversion plane at DEPTH=20m XYZ points
DDEPTH040    : Inversion plane at DEPTH=40m XYZ points
DDEPTH060    : Inversion plane at DEPTH=60m XYZ points
DDEPTH100    : Inversion plane at DEPTH=100m XYZ points
```

Each line contains the following data fields for each grid vertice:

```
X      : UTM Easting - WGS84, UTM Zone 15N (metres)
Y      : UTM Easting - WGS84, UTM Zone 15N (metres)
RES    : Resistivity (model inversion)
DEPTH  : Depth (ranged 0 - -100 metres)
```

7.3 GRIDS

Grids were prepared using Minimum Curvature interpolation with a 10m grid cell size.

In each main VLF Transmitter folder (NAA, NLK and NML), data grids are stored in sub-folder "GRIDS". Data grids correspond to the 7 inversion depth slices (surface, 5, 10, 20, 40, 60 and 100m) and are named as follows (where "xxx" is NAA, NLK or NML):

```
xxx_RES_000_FNL.grd     : final resistivity depth slice (surface)
xxx_RES_005_FNL.grd     : final resistivity depth slice (5 metres)
xxx_RES_010_FNL.grd     : final resistivity depth slice (10 metres)
xxx_RES_025_FNL.grd     : final resistivity depth slice (20 metres)
xxx_RES_040_FNL.grd     : final resistivity depth slice (40 metres)
xxx_RES_060_FNL.grd     : final resistivity depth slice (60 metres)
xxx_RES_100_FNL.grd     : final resistivity depth slice (100 metres)
```

3D grids :

3D grids (Geosoft "voxel" format) were also created and are stored in each main VLF Transmitter folder (NAA, NLK and NML) in the "VOXEL" sub-folder

7.4 README

Sub-set Archive documentation (specific to VLF_INTERP data set) : B503ARC_VLF_INTERP.ReadMe

KWAI Property Plan View with Local Features

- KWAI Unpatented Claims
- Claims Intersecting Survey
- 2019 Ground IP East and West Grids
- Pakwash Provincial park
- Cabin Bay Area
- Dixie Lake Area
- Waterbodies
- Alienations
- Elevation

1: 50,000

NAD 1983 UTM Zone 15N

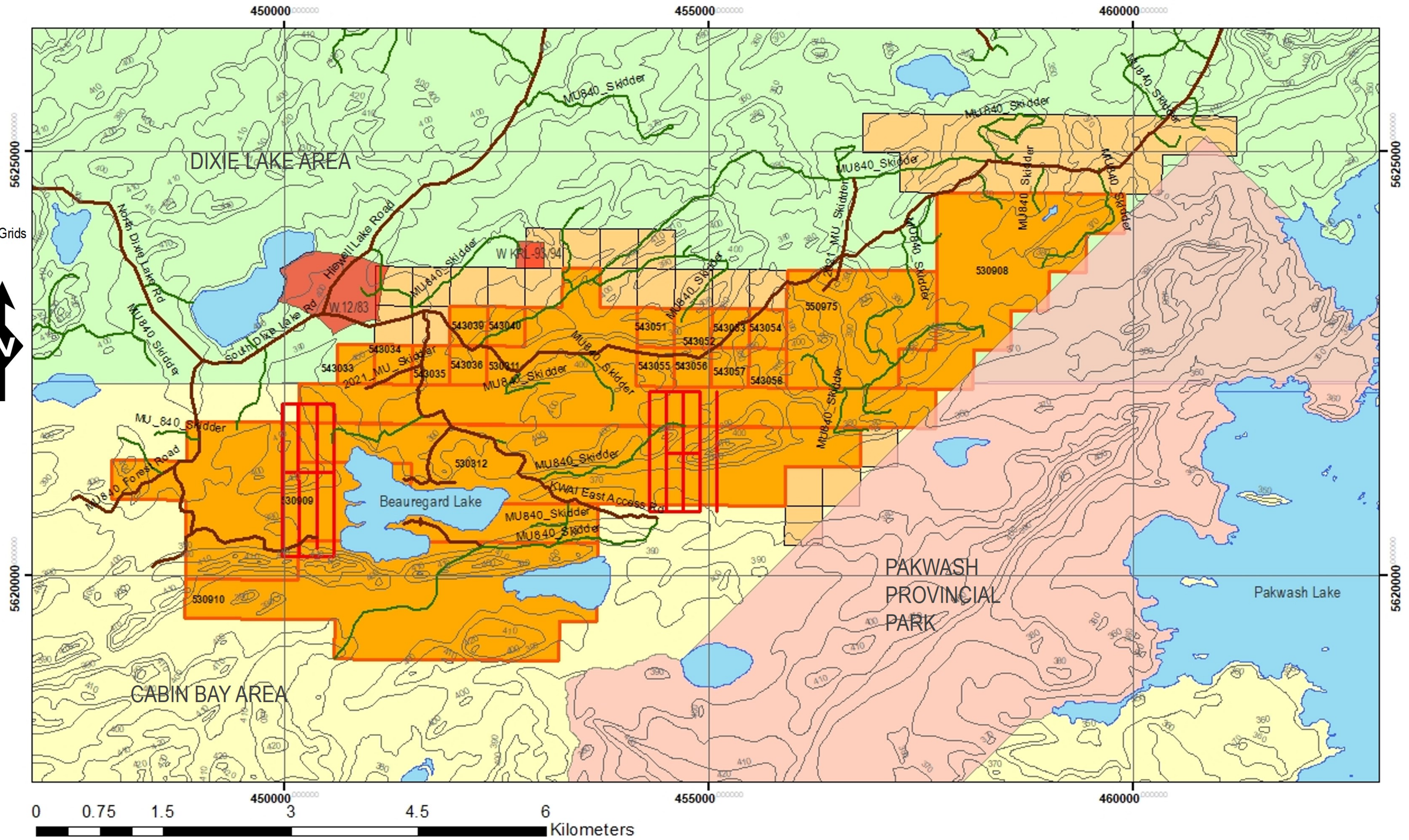

2020 KWAI Work Program Expense Totals	
Work Type- Airborne Geophysical Survey Work- cost per km	$95
Total Flight Km	$277
Ground Geophysics Survey Program Total:	**$26,234.00**